UNIVERSITY OF SOUTHAMPTON

FACULTY OF PHYSICAL AND APPLIED SCIENCES

Physics and Astronomy

Interaction of gold nanoparticles with neurons

by

Agathi Christofidou

Thesis for the degree of Master of Philosophy

2013

UNIVERSITY OF SOUTHAMPTON
FACULTY OF PHYSICAL AND APPLIED SCIENCES
Physics and Astronomy

ABSTRACT

Master of Philosophy

Interaction of gold nanoparticles with neurons

by Agathi Christofidou

In the last few decades, advances in nanotechnology have resulted in the production and use of inorganic nanoparticles (NPs). These NPs have been used commercially for a range of applications, particularly in the biomedical field, based on their exceptional chemical and physical properties, which are very different to that in the larger scale. Our understanding regarding the NP interaction with the cells following NP exposure, prior to their use it is very important. This was the motivation for the work carried out in this thesis.

Initially, the investigation presented in the thesis involved the synthesis of spherical and hollow gold NPs, which were then capped by water soluble organic oligo-ethylene glycol ligand (OEG). The OEG-capped NPs were then functionalised by attaching a specific cell targeting peptide, lysine terminated-Tet1, on their organic corona. The surface modification of the NPs by the aforementioned ligands, was carried out so that the NPs could be employed in the biological investigations carried out in this project.

PC12 and SH-SY5Y cells, neuron-like cell lines, were exposed to the synthesised gold NPs, and the fate of these NPs within the cells was studied by using transmission electron microscopy (TEM). The TEM images revealed that spheres and hollow gold NPs were found within the PC12 cells, indicating that they were able to traverse through the cell membrane. Though, the pathway and cellular processes involved could not be specifically defined due to time constrains. Furthermore, the peptide-functionalised NPs targeted the GTb1 receptors which are readily expressed on PC12 and SH-SY5Y cells. Lysine terminated Tet1-functionalised NPs uptake seemed to be greater compared to OEG-capped NPs, and they were transported to the inner part of the cell around its perinuclear region. Nevertheless, further experiments involving fluorescently tagged NPs would give us an inside on the cellular events that take place following NP exposure, over time. In addition, western blot

analysis of proteins involved in a cell stress response could give us information whether the cell is under a stress when it is exposed to gold NPs.

Furthermore, the application of the hyperspectral darkfield microscope designed by the Muskens group for imaging of single hollow gold NPs on a TEM grid and in a biological sample (with fixed SH-SY5Y cells), was also presented in this Thesis. The low illumination intensity used (<0:5 W/cm^2) is a very good aspect of this setup for future studies with living cells and gold NPs. For example, single hollow gold NPs could be used as spectral sensors of a particular cell signalling pathway.

Declaration of authorship

I, Agathi Christofidou, declare that the thesis entitled “Interaction of gold NPs with neurons” and the work presented in the thesis are both my own, and have been generated by me as the result of my own original research. I confirm that:

- this work was done wholly or mainly while in candidature for a research degree at this University;
- where any part of this thesis has previously been submitted for a degree or any other qualification at this University or any other institution, this has been clearly stated;
- where I have consulted the published work of others, this is always clearly attributed;
- where I have quoted from the work of others, the source is always given. With the exception of such quotations, this thesis is entirely my own work;
- I have acknowledged all main sources of help;
- where the thesis is based on work done by myself jointly with others, I have made clear exactly what was done by others and what I have contributed myself;
- parts of this work have been published in peer-reviewed conferences and journals (please see list of publications in the following page).

Signed: ……..

Date: …….

List of Publications-Conferences

[1] “Hyperspectral darkfield microscopy of single hollow gold nanoparticles for biomedical applications ”,
N. Fairbairn, A. Christofidou, A. G. Kanaras, T. A. Newman, and O. L. Muskens, *Phys. Chem. Chem. Phys.*, 2013.

[2] “Interaction of gold nanoparticles with neurons ”,
A. Christofidou, T. A. Newman, and A. G. Kanaras, Oral presentation and poster presentation, NanaX4, Fuengirola, Spain, 7^{th} -11^{th} of May, 2012.

Acknowledgements

Firstly, I would like to thank my MPhil supervisor Dr. A. G. Kanaras for the guidance, supervision, financial support, as well as for proof-reading this thesis. I am grateful that he has given me the opportunity to go to the Nanotechnology Oxford Summer School, the Italian Institute of Technology as well as to the NANAX4 conference. Furthermore, I would like to thank the co-supervisor of the MPhil Dr. T. A. Newman, for the supervision and financial support of the work carried out during the project. Also, I am thankful to both Kanaras and Newmans groups.

I am also grateful to Mrs Tasha Fairbairn (Muskens group) for setting up the hyperspectral darkfield microscope and for the experimental analysis she carried out. I would also like to thank Dr. Ricardo Di Corato (Italian Institute of Technology, Genoa) for his help and guidance in magnetic nanoparticle synthesis, Miss Rute Fernandes (Kanaras group) for her help in gold nanoparticle synthesis and Mrs Patricia Goggin (Biomedical Imaging Unit, Southampton General Hospital) for her help and guidance on the transmission electron microscope.

I am extremely thankful to Professor Anne Tropper for her great understanding, encouragement, and the valuable time she patiently and kindly spent listening to me. Professor Anne Tropper and Mrs Sonal Mehta, offered me unconditional support, without which I strongly believe I would not have been able to reach the end of this very challenging journey. I would also like to thank Professor Pavlos Lagoudakis, as well as my advisor Dr. Peter Lanchester for their understanding, guidance and support.

Furthermore, I would like to thank all the wonderful people that supported me during the MPhil years, especially the last few months: Father Aimilianos, Father Mehail and Father Vasileios, my great friends Peristera and Thomas, Aleksandros, Antonis and Eutychia, Chriso, Spiros and Antigoni, Ioanna, Nikos, and Anastasios. I am very grateful to them for their love, care and support, and I hope to do the same for them in the future.

I am also very thankful to my lovely family, my parents Yiannakis and Julia, my brother Christos, and my sister Aegli with her husband Tasos, who together with my husband's

family, Yiannis, Mairi, Nikos and Maria, stood by me every step of the way and with their love kept reminding me what is most important in life.

Last but not least I would like to thank my wonderful husband, Georgios, who since the beginning of our common journey, unconditionally loves, understands and supports me and without him it would not have been possible for me to complete this work. For this and for many more, I deeply love and thank him from the bottom of my heart.

Finally, I want to take this opportunity to express my full gratefulness towards God for all the people, obstacles, difficulties and opportunities, He has blessed me with in this life; they were and are all great gifts.

Table of Contents

Table of Figures

List of Abbreviations and Acronyms

CTAB	Cetyl trimethylammonium bromide
Da	Dalton
EDC	1-(3-(dimethylamino)propyl)-3-ethyl-carbodiimidemethiodide
FBS	foetal bovine serum
HS	horse serum
ICP-MS	inductively coupled plasma mass spectrometry
LSPR	localised surface plasmon resonance
NGF	neuron growth factor
NP	nanoparticle
OEG	mono-carboxy (1-mercaptoundec-11-yl) hexaethylene glycol
PBS	phosphate buffered saline
rcf	relative centrifugal force
sulfo-NHS	N-hydroxysulfosuccinimide
TEM	transmission electron microscopy
UV	ultraviolet

Chapter 1. Introduction

1.1 Inorganic Nanoparticles: Exposure and Health impact

Advances in nanoscience have resulted in the production and use of inorganic nanoparticles (NPs). NPs are commercialised for a range of applications (biomedicine, electronics, coatings, cosmetics, advanced materials and fuel additives) based on their exceptional chemical and physical properties (including optical, electronic and magnetic). The unique properties of inorganic NPs arise due to their metallic component, small size (diameter <100 nm) and controlled metrological characteristics, as opposed to the bulk material [1, 2]. NPs are highly reactive entities thanks to their high surface area compared to their core (unlike micro- and macro- particles).

The use of inorganic NPs in so many scientific fields has resulted in an exponential rise in their production. It has been estimated that between year 2011 and 2020, 58000 tonnes of NPs will be produced [3]. Nevertheless, the impact that these NPs have on health and the environment has not yet been fully explored [3]. Human exposure to inorganic NPs may happen as a result of direct application of products containing NPs, or through NP dispersion in the environment during their manufacturing processes and applications. Possible routes of NP entry into the human body, include the respiratory tract through inhalation [4], skin by translocation of NPs found in cosmetics (ZnO NPs [5]) and blood circulation by intravenous administration in nanotherapeutics (gold and magnetic NPs [6]), as illustrated in Figures 1.1 and 1.2. Cellular uptake and fate of NPs depend on their metrological characteristics, i.e. their size, charge, shape and surface coating [7, 8].

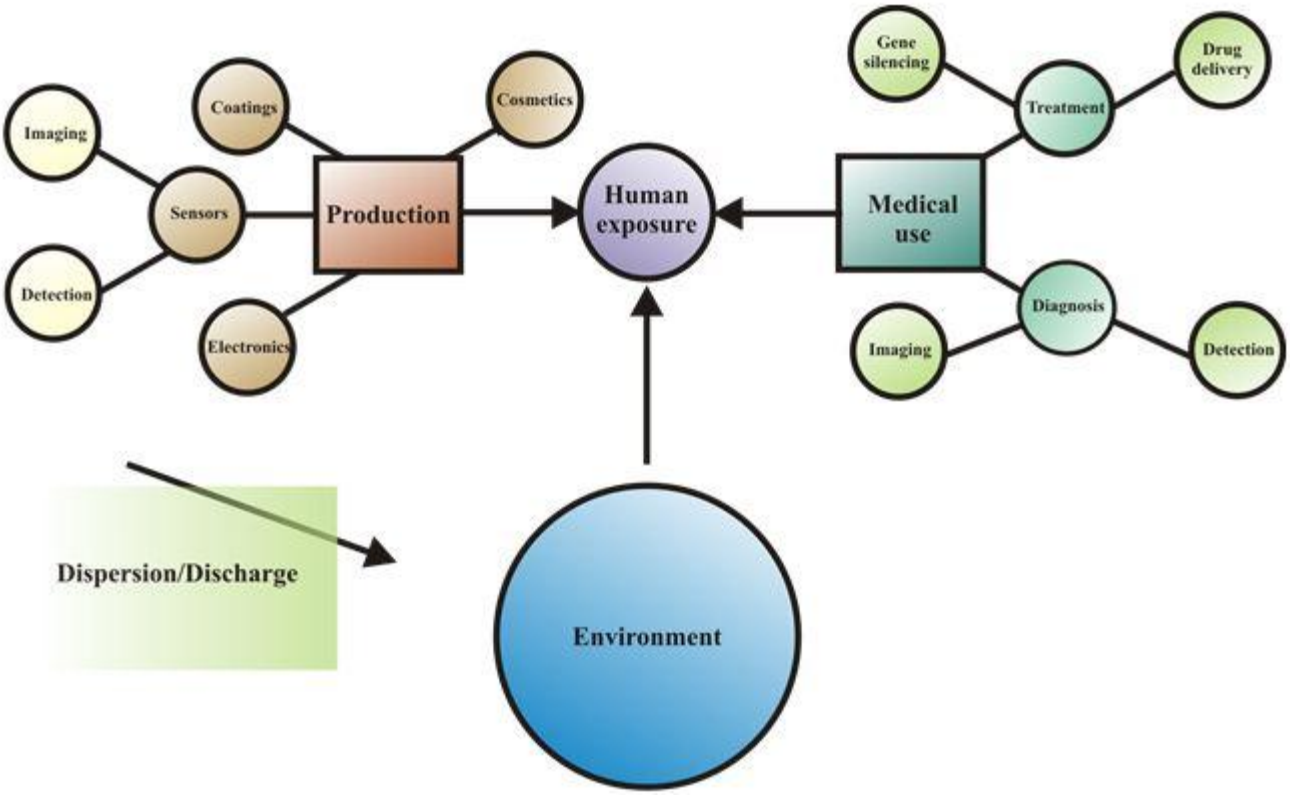

Figure 1.1. Potential nanoparticle exposure routes from the current commercialised nano-applications.

Amongst the vast majority of inorganic NPs available, gold NPs have been used extensively in research, particularly in medical therapies [9]. Gold NPs have been used previously as a model system to answer fundamental questions as to how the shape, size and functionality of particles influence their fate in cells, as well as how their metrology affects functional processes within cells [7, 10]. For example, Hutter *et al.* found that gold NPs of different morphologies (spheres, rods and branched shape) and surface coatings (poly(ethylene) glycol, PEG, and Cetyl trimethylammonium bromide, CTAB) had different effects on the immunological state of the cells (microglia cells) that constitute the innate central nervous system's immune system [11]. In another study the uptake of gold NPs by prostate cancer cells was associated with the different size (30—60 nm diameter range), shape (spheres and rods) and surface chemistry of gold NPs [12].

Information about the interaction of gold NPs with biological tissue is important considering that gold NPs are already in the first stages of clinical trials as part of patients' cancer treatment. In recent clinical trials, gold NPs have been employed as delivery vehicles

of anti-tumour agents, either directly by targeting a solid tumour (recombinant human tumour necrosis factor alpha) or by gene silencing (siRNA to specifically downregulate the expression of RRM2 gene, which is considered an anti-cancer target). This study demonstrated that anti-tumour agent side effects were reduced, due to the specific targeting of tumours and not of healthy tissue [13]. Also, the nanotherapeutics in these clinical trials resulted in a stable disease, and in slowing of tumour development for some patients. In these trials, NPs were functionalized with PEG for biostability and for evading the reticuloendothelial system. That is, PEG capped gold NPs were able to remain in the blood circulation for longer, increasing the probability of higher NP accumulation within the solid tumour. Investigation of tumour biopsies revealed that after 24 hours, gold NPs were found within the tumour tissue, as well as in healthy tissue (such as the liver of patients). In pre-clinical studies, Libutti *et al*. found that these particles had a half-life of four months in the liver [13]. Other studies using gold NPs also showed accumulation into the liver [14].

The cellular fate of gold NP following their administration, their distribution within the body and their clearance were not assessed in these clinical trials, since there are limiting factors for such an investigation in humans. Nevertheless, the impact of NPs that are deposited in tissue for a relatively long time on the different organ systems, such as the circulatory, immune and nervous systems is important and has to be assessed. In particular, the nervous system is very likely to be exposed to NPs during NP administration, since its spatial distribution within the body is in close proximity to the NP exposure sites (see Figure 1.2).

Studies about the interaction of inorganic NPs effect on neurons and the central nervous system (CNS) are limited [14, 15, 16]. Therefore, there is an increasing need for understanding the interaction of inorganic NPs and neurons.

In this work, gold NPs were chosen as a model system to study the events and consequences of inorganic NPs-biological system interaction. Gold NPs (spheres and hollow) were synthesised, capped with OEG (short PEG) layer and functionalised with a neuron targeting peptide (Lysine terminated-Tet1). Then neuron-like cell lines (PC12 and SH-SY5Y cells) were exposed to the fabricated NPs. Images obtained from transmission electron microscopy (TEM) were used to study how these NPs interacted with the cells. In addition,

the gold NP interaction with the neuron-like cells was also investigated by employing a novel optical setup, which uses hyperspectral darkfield microscopy that was developed by the Muskens group (University of Southampton). The analysis of both the NP samples, as well as the biological samples, was performed by Mrs Tasha Fairbairn.

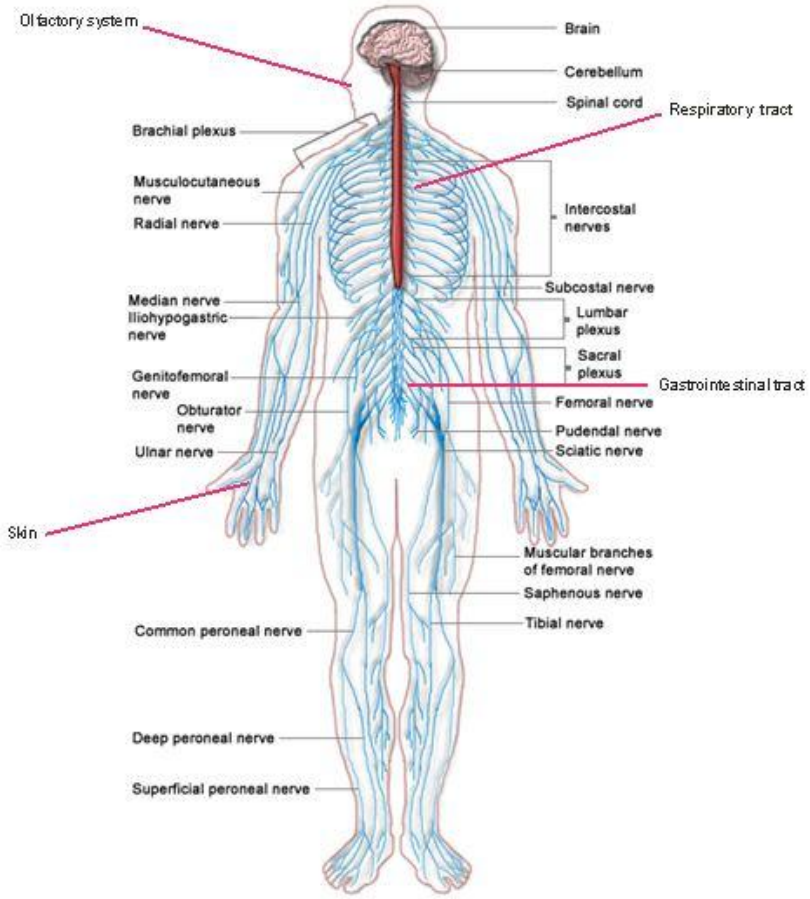

Figure 1.2. The human nervous system is in close proximity to the possible sites of inorganic NP exposure, including skin, gastrointestinal tract, as well as olfactory, respiratory and circulatory systems.

1.2 Overview of the Thesis

This Thesis investigates the interaction of inorganic NPs with neuron-like cells, and uses gold NPs as a model to understand how the different type (spherical- and hollow- shaped) of NPs, as well as the functionality of particles (OEG ligand or cell specific peptide) influence the way they interact with these cells.

The Thesis comprises of five Chapters. A theoretical background on the nervous system, and the neuron-like cell lines that were chosen to investigate the scientific questions of interest, PC12 and SH-SY5Y cells (which are considered to be good models for neurobiological investigations and share many characteristics with primary neurons), as well as on the processes of synthesis of gold NPs employed in the experiments carried out, is presented in Chapter 2. The chapter finishes with a brief reference to the hyperspectral darkfield imaging.

Chapter 3 is concerned with the detailed experimental processes involved in the preparation of morphologically sophisticated and functional inorganic NPs, as well as the development of new protocols and techniques associated with their implementation in biological studies. This chapter also includes a detailed description of the protocols employed and refined during neuron-like cell culturing of PC12 and SH-SY5Y cells. In addition, the preparation of the biological samples for transmission electron and hyperspectral darkfield microscopies is outlined in this chapter.

Chapter 4 investigates the interaction of the synthesised gold NPs with the neuron-like cell lines by imaging them with TEM. The development of gold NPs with extended functionalities with respect to biostability, imaging and neuron targeting is also discussed in this chapter. Moreover, in Chapter 4, a different approach is presented for imaging the synthesised gold NPs on a TEM grid and within biological samples prepared by the author, which was conducted through our collaboration with Muskens group. Mrs Tasha Fairbairn developed a hyperspectral darkfield microscopy setup, for imaging and spectroscopy of individual hollow gold NPs.

Chapter 2. Theoretical Background

2.1 Nervous system: overview of the system and its importance

Neurons are the major components of the nervous system. These cells are responsible for coordinating the actions of the body and for relying information between its different regions in the form of electrochemical signals.

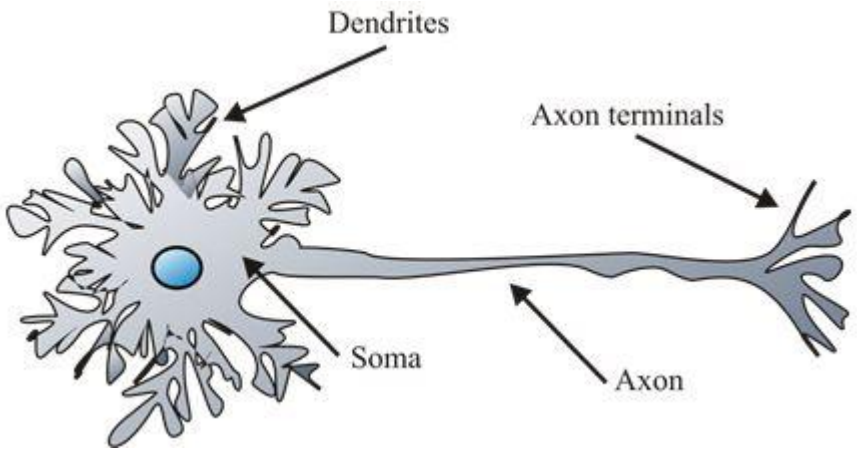

Figure 2.1. A typical neuronal cell.

Neurons are comprised of axonal and somatodendritic regions. These are distinct to each other, both spatially as well as functionally. The neuron cell soma is similar to that of a typical cell; it has the same subcellular organelles, but is capable of a high rate of protein production. Therefore, after proteins are synthesised in the cell soma they have to be transported into and along the axon cytoskeleton by axonal transport. Neurons have a high population of mitochondria (energy production organelles) as they have a high metabolic demand in order to carry out basic cellular processes, such as axonal transport.

The neuron's cellular function is highly dependent of the proper functioning of its axonal transport, consisting of a cytoskeleton and associated transport machinery, i.e. motor proteins. The neuronal cytoskeleton is made up of long polarized proteins called microtubules, which have a negative and a positive end. The cytoskeletal nanomatrix is regulated and supported by a specialised family of proteins, the microtubule-associated proteins (MAP, MAP2 and MAPT or tau). The microtubule scaffolding supports the intraneuronal transport system, which is used by molecules and organelles to move along the neuron. Their direction of travel is mainly defined by the microtubule polarity and the motor

protein involved. The axonal region is characterised by a unidirectional polarity, whereas the somatodendritic region has a bidirectional polarity [17].

2.2 Neuron cell lines

The neuronal cell lines employed in this work were PC12 cells and SH-SY5Y cells, as they are considered to be good models for neurobiological investigations and share many characteristics with primary neurons. In the presence of neuron growth factor (NGF), PC12 pheochromocytoma cells stop dividing, then differentiate into neuron-like cells, and extend neurites which are highly branched (see Figures 4.1 and 4.2). Once differentiated, they have neuron cell properties (similar to primary sympathetic neurons) and express receptors for nicotinic acetylcholine, choline acetyltransferase, GABA and tyrosine hydroxylase. PC12 cells can also produce and excrete dopamine and noradrenaline (neurotransmitters) [18]. They are considered to be a good neurobiological and neurochemical model system, for example, in investigations of mechanisms involved in the neurite outgrowth, as well as the synthesis and release of neurotransmitters [19, 20].

SH-SY5Y neuroblastoma cells, in the presence of retinoic acid, are able to differentiate into cells with neuron-like properties. The differentiated SH-SY5Y cells possess characteristics of primary neuronal cells, as they express neuronal markers, and have neuronal filaments, neuronal polarity markers (tau and MAP-2 proteins) and GAP-43 protein. Also, they are able to respond to neuronal growth factors, such as brain derived neurotrophic factor [21]. The differentiated SH-SY5Y cells can serve as a model for studying the mechanisms of a damaged axonal transport system, characterised by destabilization of the microtubule scaffolding [22].

2.3 Physicochemical properties of metallic NPs

As discussed earlier in Chapter 1, metallic NPs are used in a wide range of applications which are based on their exceptional physicochemical properties. These properties of inorganic NPs arise mainly due to their metallic component and small size (10^{-9} m),

compared to the bulk material [1, 2]. In noble metal NPs (such as gold NPs) with a diameter smaller than the wavelength of light (λ), a unique optical phenomenon is observed, the localised surface plasmon resonance (SPR) [23, 24]. SPR arises when the NPs are subjected to an electromagnetic field at a particular frequency, and as a consequence the metal free electrons oscillate collectively and in a resonant frequency with the electromagnetic wave. These resonant, collective oscillations have as an effect the enhancement of the absorption and scattering, extinction, of the electromagnetic field in resonance with the NPs SPR frequency, from which the unique optical properties of noble metal NPs arise.

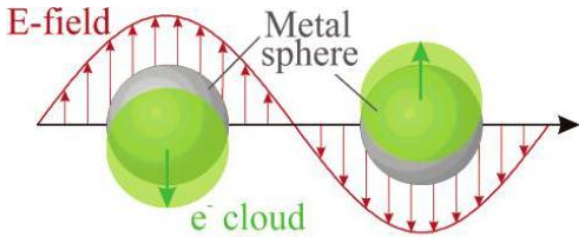

Figure 2.2. An illustration of the plasmon oscillation of metallic spherical NPs. The electron charge (e-) cloud is displaced relative to the nucleus **[23]**.

Some of the factors which control the SPR, include the size and shape of the NPs, and electric properties of the medium that the NPs are embedded; as suggested by the Mie theory [23, 24].

According to Mie theory, when the radius of the NPs, R, is much smaller than λ, then the extinction cross-section can be expressed as below,

$$C_{ext} = \frac{24\pi^2 R^3 \varepsilon_m^{3/2}}{\lambda} \frac{\varepsilon''}{(\varepsilon' + 2\varepsilon_m)^2 + \varepsilon''^2}$$

Equation (2.1)

where ε_m is the dielectric constant of the embedded medium, and ε'(λ) + iε" (λ) is the NPs dielectric function. Furthermore, the NPs (spheres) maximum extinction takes place, at λ, as an individual plasmon band, whereby ε' = - 2ε_m. On the other hand, the SPR of NPs with a different shape, like hollow, can be obtained by other mathematical methods, for example discrete-dipole approximation of Mie's theory [25, 26]. Moreover, by employing the

discrete-dipole approximation of Mie's theory, it is shown that the SPR of the hollow gold NPs depends on the radius of the NPs as well as the thickness of the NPs shell.

As mention earlier in this section, the LSPR of gold NPs depends on the NPs size, thus by tuning the size of gold NPs their LSPR can also be controlled. For example, spherical gold NPs with a small diameter (20nm), absorb the light (almost) completely, with insignificant scattering. As their size increases the contribution of the absorption component to the overall excitation spectra decreases, whereas the contribution of scattering increases [24]. Therefore, NPs of the appropriate size can be used, accordingly, in the most suitable optical imaging applications. Such an example, are large NPs (like hollow gold NPs) which can be employed in light-scattering imaging setups.

2.4 Synthesis of inorganic nanoparticles

Gold hollow (Section 2.4.1) and spherical (Section 2.4.2) NPs were synthesised by wet chemistry processes. The theoretical background of these synthetic processes will be described below.

2.4.1 Hollow gold nanoparticles

The preparation of hollow gold NPs involved the synthesis of spherical silver NPs, followed by a galvanic replacement reaction, during which the gold ions ($AuCl^-_4$) were reduced into Au^0, whereas silver was oxidised to Ag^+ ions (Equation 2.2). A single gold atom replaced three silver atoms resulting to the formation of hollow gold nanoparticles (Scheme I) [27].

$$3Ag_{(s)} + AuCl^-_{4\,(aq)} \longrightarrow Au_{(s)} + 3Ag^+_{(aq)} + 4Cl^-_{(aq)}$$

Equation (2.2)

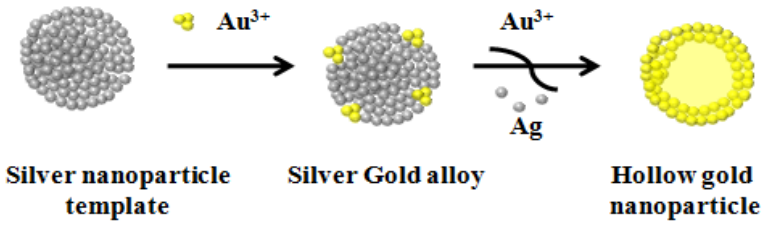

Scheme I

2.4.2 Spherical gold nanoparticles

The spherical gold NPs were synthesised by the well-established Turkevish method, whereby Au^{3+} is reduced by trisodium citrate [28].

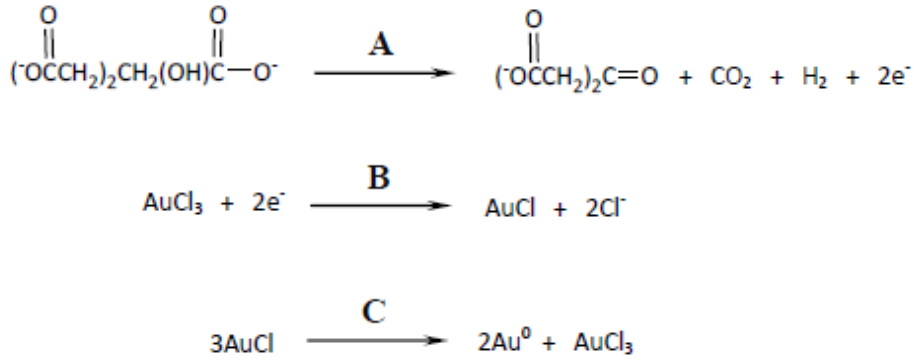

Figure 2.3. Scheme showing the different steps involved in the formation of spherical gold NPs: A. oxidation of trisodium citrate, B. reduction of $AuCl_3$, and C. disproportionation of AuCl **[28]**.

In [28] is suggested that three steps, illustrated in Figure 2.3, take place in series and parallel, during the spherical gold NP synthesis. Firstly, oxidation of citrate anions, by oxygen in air, takes place, and as a result dicarboxy acetone is formed. Furthermore, Au^{3+} ions are reduced to Au^{+} cations. The dicarboxy acetone forms complexes with Au^{+} cations (three Au^{+} cations bind to a minimum of two dicarboxy acetone moieties). The dicarboxy acetone plays a key role in nucleation. Also, the Au^{+} cations disproportionate to Au^{0}, which then adsorb to Au^{+} cations, and as a result large complexes are formed. Finally, nucleation takes place when these large complexes reach a critical size of 2 nm (according to [28]). Then the nuclei formed grow into NPs, as the Au^{0} (in the solution) are absorbed by the nuclei. The trisodium citrate present in the solution, provides stability to the growing NPs.

2.5 Surface capping and functionalisation of the nanoparticles

2.5.1 Oligoethylene glycol capping of gold nanoparticles

NPs were coated with the OEG ligand via its –HS group.

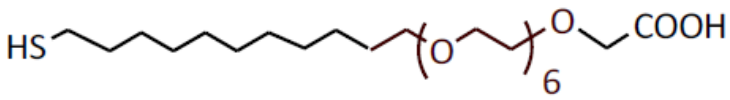

Figure 2.4. The chemical structure of the OEG ligand (SH-OEG-COOH).

The OEG-capping provides stability to the gold NPs when they enter an environment high in salt and proteins, which is considered to be very challenging for the NPs to stay in a colloidal form. According to [29], this is achieved via the hydrophilic (-(EG)$_6$-OCH$_2$-COOH) part and the hydrophobic (C$_{11}$) carbon chain of the ligand, which gives the NPs, solubility and stability, respectively. Furthermore, the (-(EG)$_6$-OCH$_2$-COOH) unit of the ligand, also allows further modification of the NPs surface by ligands containing amine, such as peptides.

2.5.2 Peptide functionalisation of gold nanoparticles

The peptide functionalization involves a straightforward coupling method, whereby carboxyl groups couple to primary amine groups, in the presence of a zero-length cross-linker, 1-(3-(dimethylamino)propyl)-3-ethyl-carbodiimidemethiodide (EDC) [30].

Firstly, a reaction between EDC with a carboxylic group takes place which results in the production of O-acylisourea. O-acylisourea is an amine reactive intermediate which i. Reacts with an amine or ii. Hydrolyses to generate a carboxyl. In an order to avoid the latter, N-hydroxysulfosuccinimide (sulfo-NHS) is employed, so as to rise the reaction's efficiency. That is by stabilising O-acylisourea, as it converts it to sulfo-NHS ester which is amine reactive [30].

A neuron targeting ligand, lysine terminated-Tet1 peptide (peptide sequence: KHLNILSTLWKYR), was chosen to induce the delivery of gold NPs into the cells, as it can mediate a specific as well as an enhanced binding of nanostructures (such as polymersomes

[31]) or non-viral vectors, on differentiated PC12 cells, differentiated SH-SY5Y cells, dorsal ganglion neurons and primary motor neurons [32, 33, 34]. The membrane of these cells expresses an acidic glycolipid, GTb1 ganglioside, which acts as a receptor for Tet1 [35]. This neuron-targeting peptide it has similar binding characteristics to that of tetanus toxin [34], and enables functionalised nanostructures to enter the cells by first binding onto the cellular surface and then undergo retrograde transport from the neurites to the cell soma [32].

In Section 3.2.2, a detailed protocol of Tet1 peptide functionalization of the gold NPs is presented.

2.6 Hyperspectral darkfield microscopy

Over the last few years, a great effort has been put in developing advanced imaging techniques for producing images of single non-fluorescent inorganic metallic NPs [36], which could extend and complement the knowledge in the biomedical science field currently obtained from other microscopic techniques (such as fluorescence microscopy).

A powerful technique for imaging and spectroscopy of inorganic metallic NPs (diameter > 20 nm), detects the light that is elastically scattered by these particles and is called darkfield microscopy [37, 38]. Furthermore, darkfield spectroscopy (together with the metallic NPs SPR's high sensitivity to small alterations in the local environment) has been broadly employed for sensing [39]. A broadband single NP spectroscopy results in fast and/or high resolution of a single NP, but it has a few drawbacks in the context of biological imaging studies. This is because the metallic NPs which interact with a biological sample are heated up from the broad spectrum of irradiation [40, 10].

In the hyperspectral darkfield microscopy setup developed by Muskens group, a spectral imaging of a large area with fast integration times has been made possible by a combination of a standard darkfield microscopy setup with a spectrally filtered source. This setup is presented in detail in [41], and as mentioned earlier, in Chapter 4 its application in carrying out spectral measurements of hollow gold NPs and of biological samples, synthesised and prepared, respectively, by the author.

Chapter 3. Methods and Techniques

3.1 Synthesis of inorganic nanoparticles

3.1.1 Hollow gold nanoparticles

Hollow gold NPs were prepared using spherical silver NPs as templates, followed by a galvanic replacement reaction. The silver template growth solution was prepared by stirring CTAB (0.2 M, 80 ml), silver nitrate (0.05 M, 400 μl) and L-ascorbic acid (0.1 M, 2 ml) at 35 °C. It is important to note that the L-ascorbic acid solution has to be prepared just before the process of synthesis. Since L-ascorbic acid oxidises readily when it is exposed in air and light [42].

Firstly, silver NPs were synthesised (as seeds), separately, by silver nitrate (2.5 mM, 1 ml) reduction in the presence of trisodium citrate (2.5 mM, 1 ml), Milli-Q water (8 ml) and ice-cold sodium borohydride (0.001 M, 25 μl). These silver seeds (400 μl) were then injected to the reaction mixture, followed by addition of sodium hydroxide solution (1 M, 2 ml). A colour transition was observed from colourless to orange−yellow, signifying the formation of silver NPs. The reaction was completed after 24 hours, and the final product was purified from excess CTAB, by one centrifugation-decantation step (2500 rcf, 15 minutes) and re-dispersed in Milli-Q water (40 ml).

The hollow NPs were formed by a slow, constant addition of sodium tetrachloroaurate (III) dihydrate aqueous solution (1 mM, 0.25 ml) to a silver template solution (10 ml), which was heated to reflux. There was a colour transition from orange−yellow to deep blue, indicating the formation of hollow gold NPs. The NP solution was left to cool down to room temperature and was stored at 4 ^{o}C.

3.1.2 Spherical gold nanoparticles

Spherical gold NPs were synthesised by the citrate reduction method. A trisodium citrate solution (2.5 ml, 19.5 mM) was mixed with a sodium tetrachloroaurate (III) dihydrate solution (0.5 mM, 25 ml), at boiling temperatures and under vigorous stirring, leading to the formation of spherical NPs. There was a colour change from pale yellow to wine red. Once the reaction mixture was cooled to room temperature, it was then purified by filtration (0.45

μm filter, Millipore). The citrate gold NPs (27.5 ml) were then electrostatically stabilised with bis(p-sulfonatophenyl)-phenyl phosphine dehydrate dipotassium salt (10 mg) capping ligand. After two hours of stirring at room temperature, the NPs were precipitated by the addition of sodium chloride (50 mg) and purified by one step of centrifugation-decantation (2500 rcf, 5 minutes). The NPs were redispersed in Milli-Q water.

3.2 Surface capping and functionalisation of the nanoparticles

3.2.1 Oligoethylene glycol capping of gold nanoparticles

A short polyethylene glycol (PEG) ligand, oligoethylene glycol (OEG), was used to functionalize the outer surface of gold NPs, so that they would stay in a colloidal form when they enter the cell media. This means the NPs do not precipitate out, but they disperse nicely in the media. A fresh OEG-COOH solution (5 mg/ml, 200 μl) was prepared and injected into a colloidal solution of (i) spherical gold NPs (5 nM, 10 ml) while stirring and was left to react for two hours at room temperature, or (ii) hollow gold NPs (0.5 Optical Density, O.D., 5 ml) while sonicating at 4 ^{o}C for one hour. The reaction mixture was kept overnight at 4 ^{o}C and then purified from the excess ligand by three purification steps (8000 rcf, 15 minutes per step). NPs were re-dispersed in sodium borate buffer (0.1 M, pH 9).

3.2.2 Peptide functionalisation of gold nanoparticles

A neuron targeting peptide, lysine terminated-Tet1 (peptide sequence: KHLNILSTLWKYR) was conjugated to the OEG-capped gold NPs in the presence of EDC and s-NHS coupling agents. Namely, the peptide (100 μl, 0.15 mM; 0.1 M sodium borate buffer, pH 9) was added to 5 ml of gold NPs (0.3 O.D.; 0.1 M sodium borate buffer, pH 9), followed by the addition of EDC (50 μl, 0.2 M) and sulfo-NHS (100 μl, 0.2 M), and shaken gently overnight at room temperature. The peptide functionalised-NPs were purified from excess peptide ligands and coupling reagents by three purification steps (13,400 rcf, 15 minutes per step), and re-dispersed in 100 μl of cell growth media.

3.3 Characterisation techniques of inorganic nanoparticles

The NPs were characterised with UV-Visible spectra and transmission electron microscopy (TEM). The UV – Visible spectra of the colloidal NPs were obtained using Cary 100 UV-Vis spectrophotometer, in the range of 450 to 800 nm. TEM images were taken with a Hitachi H7000 transmission electron microscope operating at a bias voltage of 100 kV. The TEM specimen preparation involved deposition and evaporation of a drop of the NP solution on a grid (carbon-copper coated 400 mesh). The average size distribution of NPs was determined by analysing the TEM images of the NPs, and the data was presented in histograms (see Chapter 4).

3.4 Cell culture

The chemicals used in cell culturing processes, described in this section, were purchased from Sigma Aldrich, and culture media and components were purchased from Invitrogen-Gibco.

3.4.1 PC12 cell culturing

PC12 cells were maintained in RPMI (Roswell Park Memorial Institute) cell media which was supplemented with penicillin/streptomycin, 7 % horse serum (HS), 7 % heat-deactivated fetal bovine serum (FBS), and D-glucose in a humidified atmosphere of 5 % CO_2 and 95 % air at 37 °C. For the experiments, cells were seeded in a 24-well plate on glass coverslips (pre-coated with poly-D-lysine), at a density of 2 x 10^4 cells per well. The following day, cells were differentiated by exchanging their media from rich to low serum media (1 % of HS, 1 % of FBS), supplemented with 5 µl of neuron growth factor (NGF, 50 ng/ml). PC12 cells required seven days to fully extent their neurites.

3.4.2 SH-SY5Y cell culturing

SH-SY5Y cells were maintained in F-12 cell media, which was supplemented with penicillin/streptomycin, non-essential amino acids and 5 % FBS, in a humidified atmosphere

of 5 % CO_2 and 95 % air at 37 °C. They were seeded in a 12-well plate on glass coverslips, at a density of 2 x 10^4 cells per well, in 1 ml supplemented cell media. The following day, cells were differentiated by the addition of retinoic acid (1 μl, 3 μg/ml).

3.5 Exposure of inorganic nanoparticles to neurons

3.5.1 Preparation of biological samples for transmission electron microscopy imaging

In the first experiment (see Section 4.3) the PC12 cells were incubated with OEG capped spherical (5 nM) or hollow (1 O.D.) gold NPs, for six hours. In the second experiment, PC12 cells were incubated with OEG-capped or lysine terminatedTet1-functionalised spherical gold NPs (5 nM), for one hour.

The samples were then washed three times with pre-warmed (at 37 °C) phosphate buffer saline (PBS) pH 7.4, then incubated for 20 minutes with the fixative, 2 % paraformaldehyde/1.5 % glutaraldehyde in RPMI media containing HEPES buffer (20 mM, pH 7.4), which had been also pre-warmed at 37 °C. The cells were then washed twice in 0.1 M sodium cacodylate (pH 7.2—7.4). Sodium cacodylate was removed, and osmium mixture (1.5 % of potassium ferricyanide mixed with 1% of osmium) was added to the cells for one hour at 4 ^{o}C. The samples were washed several times in 0.1 M sodium cacodylate and dehydrated stepwise in ethanol; in each step the samples were incubated with ethanol, twice, for five minutes (30 % ethanol, 50 % ethanol, acetate uranyl in 70 % ethanol, incubated for 40 minutes, then in 70 % ethanol, 95% ethanol and finally in absolute alcohol twice for 15 minutes). Samples were then incubated in a 50:50 mixture of acetonitrile and TAAB© resin (overnight), followed by an exchange into neat TAAB resin for six hours. The cover slips were then removed from the resin, and mounted onto capsules of previously polymerised resin. These were then polymerised overnight, at 65^{o}C. The cover slips were detached from the capsules by freezing them in liquid nitrogen and breaking them off. The samples embedded in resin were then sectioned using a microtome. Lead citrate was used for post embedding staining of sections on a TEM grid. A drop of lead citrate was put on parafilm in a petri dish that had sodium hydroxide pellets in it. The sodium hydroxide acted

hydroscopicaly to prevent precipitation of lead carbonate. The grid was then inverted on the drop, covered with a lid and left for five minutes. The grid was then washed quickly with distilled water and the excess water was blotted off. Samples were then imaged with the transmission electron microscope.

3.5.2 Preparation of biological samples for hyperspectral darkfield imaging

SH-SY5Y cells were incubated with hollow gold peptide-functionalised NPs for one hour (1 O.D.), and then washed three times with PBS, pH 7.4. The samples were fixed by 15 minute incubation with 4 % paraformaldehyde. All reagents were pre-warmed at 37 $^{\circ}$C, to achieve good fixation of the samples. The fixative was then removed by washing the samples three times with PBS, followed by water. The glass coverslips were washed again with plenty Milli-Q water (excess water was blotted off) and then mounted with 4', 6-diamidino-2-phenylindole (DAPI, a fluorescent dye which stains the cell nuclei) mounting media onto a glass microscope slide.

Chapter 4. Interaction of gold nanoparticles with neurons

4.1 Neuron cell lines

4.1.1 Neuron–like PC12 cell line

The PC12 cells were seeded carefully, so that they would spread evenly, and adhere nicely, on the glass coverslip. This was very important for the cells to form nice connections with each other (see figure below). The number of the cells seeded was also important, as a high number of cells would lead to the formation of clumps resulting in the death of the cells at the base of the clump. Moreover, if cells were in small numbers they would not be able to form connections with each other, and again they would not survive. Therefore, the seeding method prior to differentiation was very important.

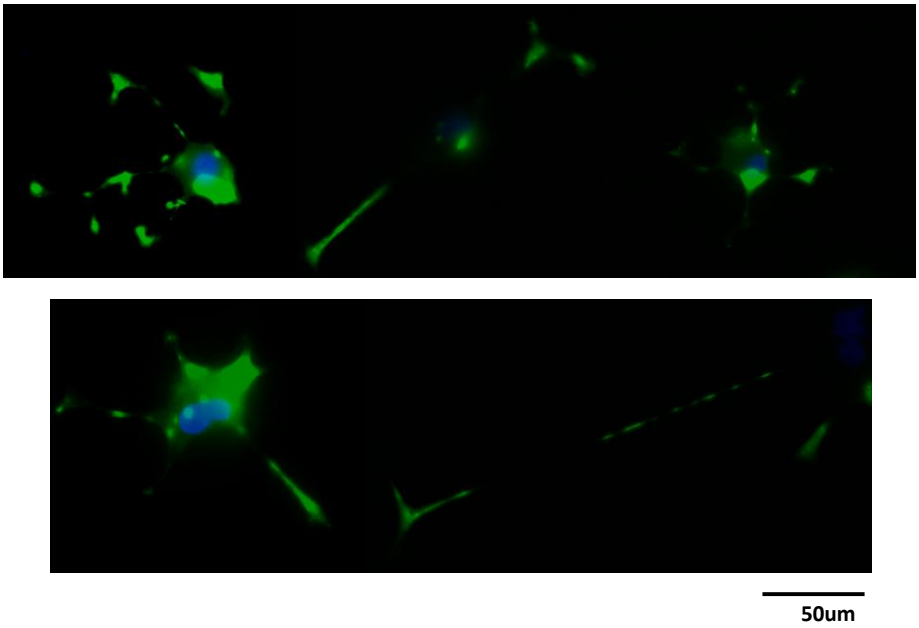

Figure 4.1. Fluorescence images of differentiated PC12 cells (at day 5 of differentiation); green βIII-tubulin staining counter-stained with DAPI, blue.

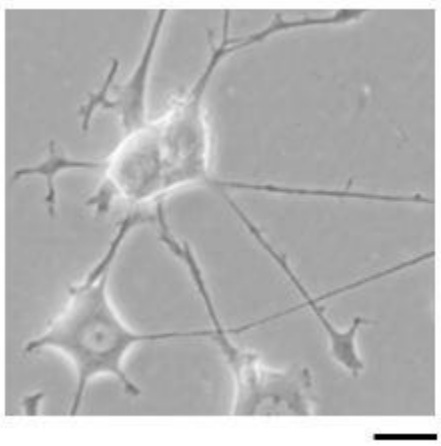

Figure 4.2. Brightfield image of differentiated PC12 cells. Scale bar = 20μm.

After the cells were seeded, they were given enough time to adhere (24 hours), before they were induced to differentiate, and start projecting out neurites. Undifferentiated PC12 cells are not able to differentiate if they do not adhere properly on a substrate [43]. For PC12 cells to fully form an extensive network with each other, so that they could be used in the experiments with NPs, they were left for a week in the presence of NGF and low serum media. These cells were very delicate, hence extensive handling could easily induce their death. On the other hand, SH-SY5Y cells were much easier to handle and used in experiments, compared to PC12 cells.

4.1.2 Neuron–like SH-SY5Y cell line

The SH-SY5Y cells is another neuron-like cell line, which is considered easier to handle than PC12 cells. They can adhere to surfaces and proliferate over time better and faster compared to other neuron cell lines. SH-SY5Y cells were left to adhere onto the seeding surface overnight and were then induced to differentiate in the presence of retinoic acid. A nice well networked cell culture was ready after four days of differentiation (see Figure 4.3).

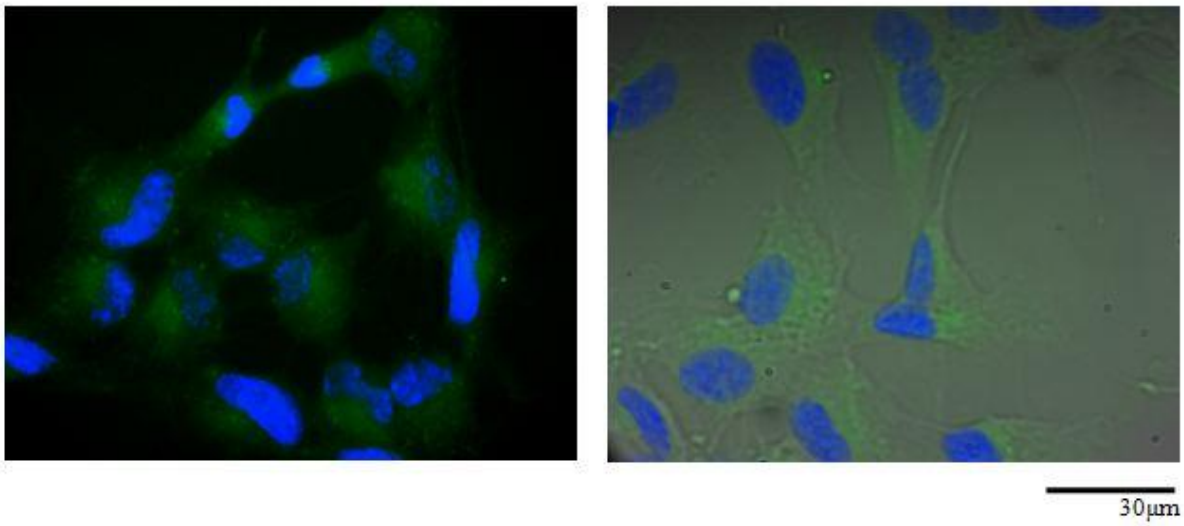

Figure 4.3. A. Fluorescence image of differentiated SHSY-5Y cells, B. An overlay of a brightfield image with fluorescence image of differentiated SH-SY5Y cells.

4.2 Gold nanoparticles

4.2.1 Spherical gold NPs

The gold spherical NPs synthesised by the Turkevich method (see Section 2.3.2) and stabilised by the ligand exchange reaction had an average diameter of 15 nm (Figure 4.4). The sharp LSPR peak at 520 nm indicated the monodispersity of the synthesised gold NPs, as well as that were stable and did not form any aggregates.

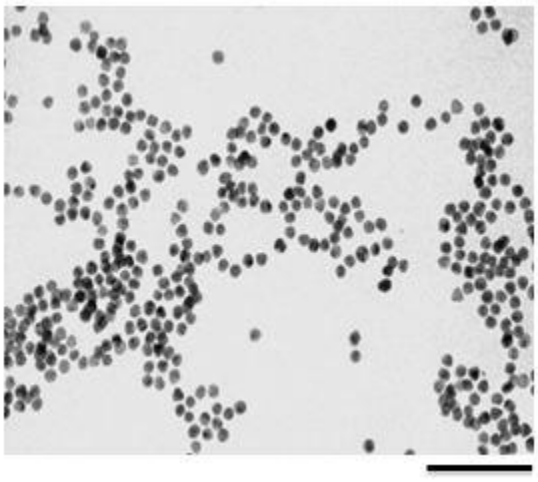

Figure 4.4. TEM image of spherical gold nanoparticles. Scale bar = 100 nm.

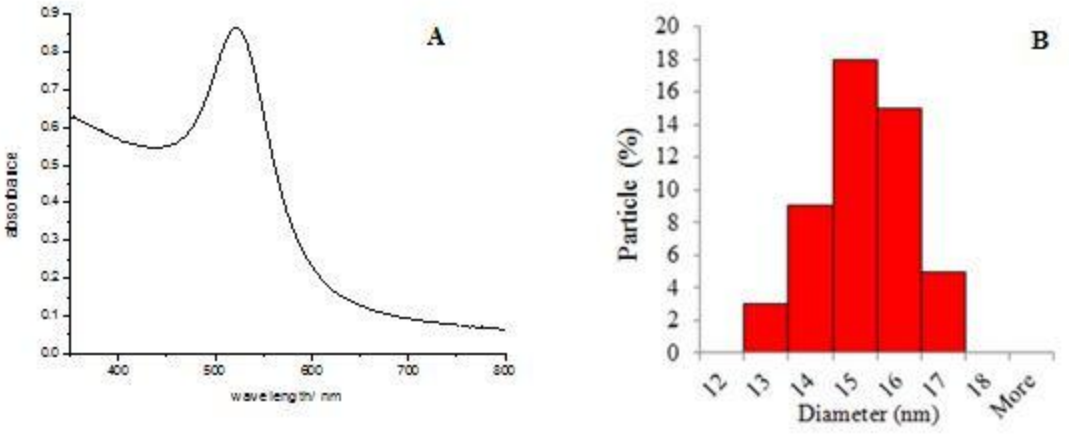

Figure 4.5. A. UV-vis spectrum of spherical gold nanoparticles and B. a histogram of the size distribution of spherical gold nanoparticles.

4.2.2 Hollow gold NPs

The preparation of hollow gold NPs involved the synthesis of spherical silver NPs, followed by a galvanic replacement reaction. The hollow gold NPs prepared by the galvanic replacement reaction had an almost rounded shape (Figure 4.6.), with an average size of 70 nm and a SPR peak at 700 nm.

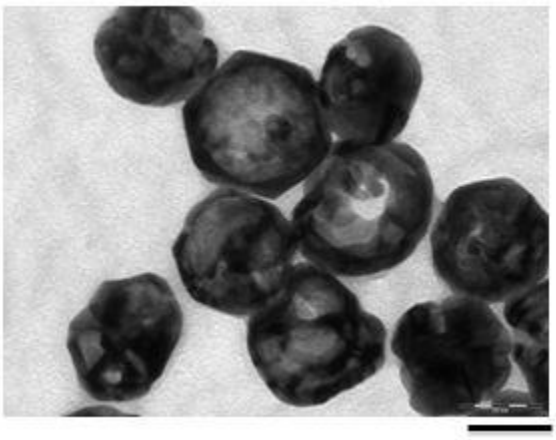

Figure 4.6. TEM image of hollow gold nanoparticles. Scale bar = 50 nm.

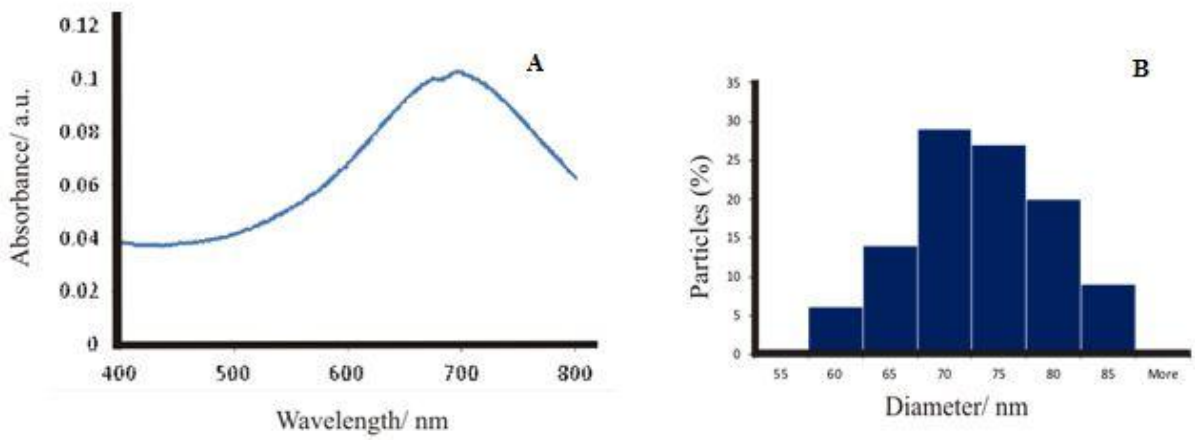

Figure 4.7. A.UV-visible spectra, and B. size distribution of the hollow gold NPs.

The TEM images and the size distribution of spherical gold and hollow gold NPs showed evidence of good NP monodispersity.

Looking Figure 4.5A and Figure 4.7A, it can be observed that the LSPR peaks of gold spheres and hollow NPs are different. These optical spectra are characteristic for each type of gold NP, as (in general) each type of noble metal NP has a unique optical signature which enables scientists to employ a particular NP to the application of interest [44, 45] (see Section 2.3). For example, in photothermal cancer therapy hollow gold NPs (instead of other type of NPs) have been employed as heat transfer agents, as their LSPR is close to the near-infrared region (and could be shifted even more towards that region by increasing their size) [26].

4.2.1 Peptide functionalisation of gold nanoparticles

As mentioned in Chapter 3, the gold NPs were capped with the OEG ligand, and then were functionalised with the neuron targeting peptide, lysine terminated-Tet1. The figure below is a schematic of the different stages of NP capping and functionalization, with the OEG and Tet1, respectively.

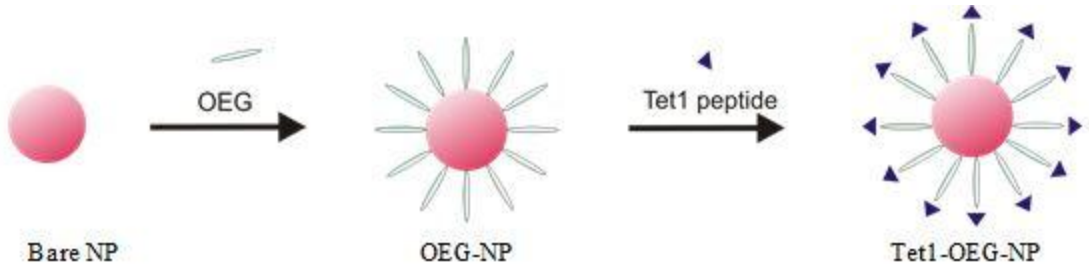

Figure 4.8. OEG capping followed by peptide functionalisation of gold NPs.

The OEG-capped NPs did not aggregate when they entered an environment that was high in salt and proteins (such as the cell media). This is because the OEG-capping provided stability to the NPs, via the hydrophilic (-$(EG)_6$-OCH_2-COOH) part and the hydrophobic (C_{11}) carbon chain of the ligand [29], which gave the NPs, solubility and stability, respectively (see Figure 2.4 for the chemical structure of the OEG ligand). Furthermore, the (-$(EG)_6$-OCH_2-COOH) unit of the ligand, also provided the NPs with functional carboxylic groups.

The peptide functionalization of the NPs, as illustrated in Figure 4.9, resulted in a red shift in the LSPR of gold NPs. This could be attributed to a change in the refractive index, as a consequence of the new layer formed by the addition of the peptide ligand around the NPs [46]. In addition, the sharp LSPR peak of the peptide functionalised NPs suggested that the NPs did not aggregate, which was consistent with the TEM image (shown in Figure 4.9).

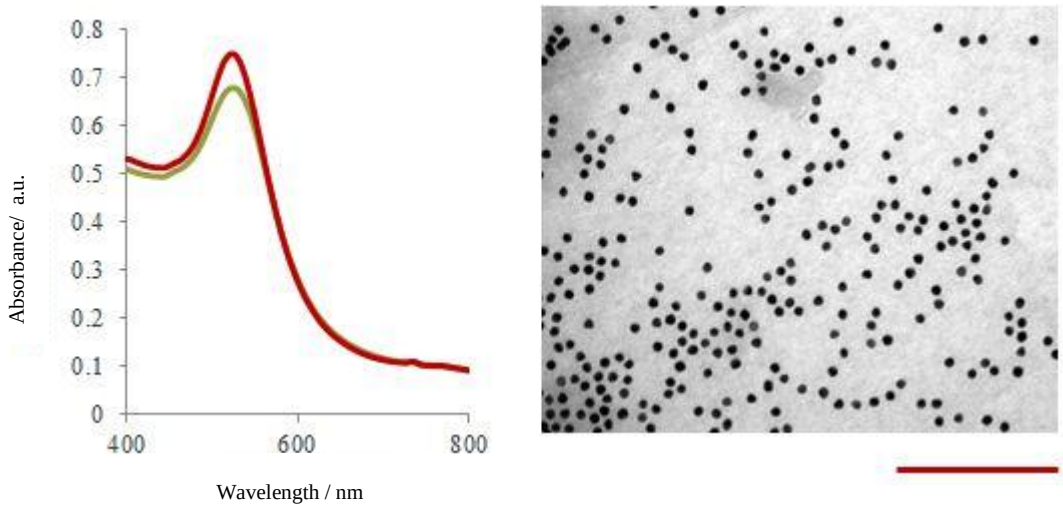

Figure 4.9. UV-visible spectra of the OEG-capped NPs (red line) and the Tet1-OEG capped NPs (green line), and TEM image of the Tet1-OEG coated NPs (scale bar = 200 nm).

Moreover, the hollow gold NPs did not precipitate out during the functionalization process with the peptide, too. They stayed in a colloidal form, which can be confirmed by the TEM images and the UV-visible spectra of the particles (see Figure 4.10). A red-shift was observed when the UV-visible spectra of the peptide functionalised NPs were plotted.

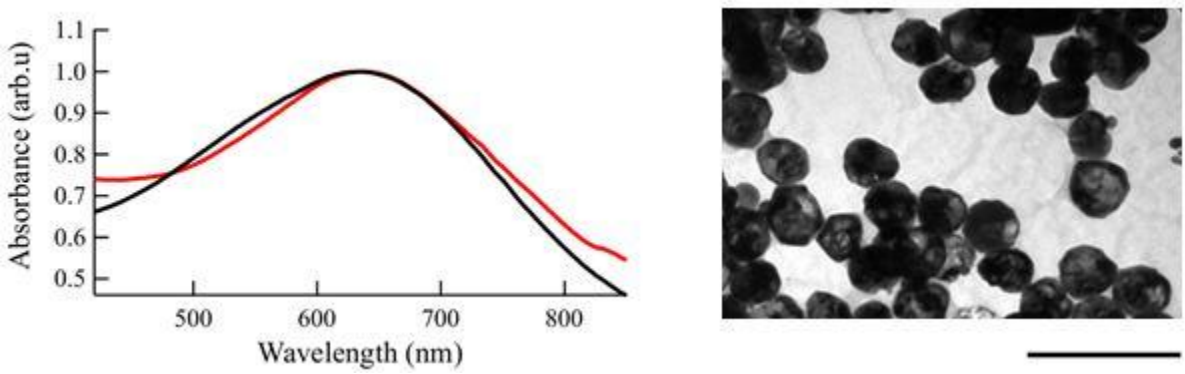

Figure 4.10. a. The UV-visible spectra of the hollow OEG-capped NPs (black line) and b. the hollow Tet1-OEG capped NPs (red line), and TEM image of the hollow Tet1-OEG coated NPs (scale bar = 200 nm).

The Tet1 peptide is slightly hydrophobic, as it is illustrated by the hydropathy plot in Figure 4.11. Therefore its attachment on gold NPs was tricky, as the reaction had to reach completion without the NPs precipitating out from the solution, and hence the ideal conditions of attachment described in Section 3.2.2, had to be found.

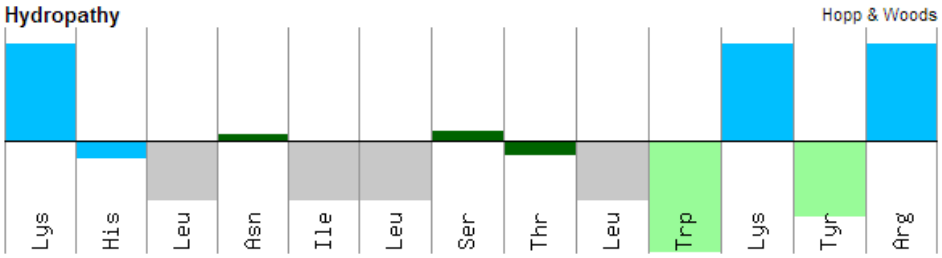

Figure 4.11. Hydropathy plot of lysine terminated-Tet1 peptide; blue= basic, green= polar, grey= aliphatic, light green= aromatic.

4.3 Cellular fate of gold nanoparticles in PC12 cells

The motivation for the work presented in this Thesis, as described in Chapter 1, was to investigate the interaction of inorganic NPs (more specifically gold), with neuron cells, in an attempt to gain more knowledge regarding the NP-cell interface, as a result of our exposure to NPs in our daily life [9]. This study involved the exposure of neuron-like cells to gold NPs, that were either OEG-capped or peptide-functionalised, and to investigate the fate of the NPs within the cells by using imaging techniques, such as transmission electron and hyperspectral darkfield microscopy.

Differentiated PC12 cells were incubated with spherical and hollow gold NPs capped with OEG, in order to assess the uptake and fate of gold NPs within the cells. A firm OEG coating surrounded these gold NPs (see Figure 4.8), to ensure their biostability in cell serum media that were rich in protein and salts [47]. This surface capping of gold NP makes them biocompatible, because the cell and its components are not exposed directly to the highly catalytic metallic surface of the gold NPs. These OEG capped NPs were expected to enter the cell in low numbers, compared to NPs that were functionalised with a cell targeting ligand [47, 10]. In this work, the experimental findings regarding the cell interaction and uptake of NPs, was drawn based on the qualitative data obtained from TEM images. Therefore, to validate these findings and construct a complete picture, further experiments are needed, and as due to time constrains these were not possible in the current project. The actual concentrations of gold NPs within cells could be quantified with accuracy by a standard technique, the inductively coupled plasma-mass spectrometry (ICP-MS). The gold NPs were easily identified within a cell using a transmission electron microscope, due to their dense electron contrast (see Figure 4.12). TEM images revealed that spheres and hollow gold NPs were found within the cell, indicating that some of them were able to traverse through the cell membrane. Moreover, it was observed that hollow gold NPs seemed to be able to enter the cell in relatively lower amounts, compared to spherical NPs. This could be attributed to their size difference, as hollow gold NPs were much bigger (70 nm) than the spherical (15 nm) gold NPs.

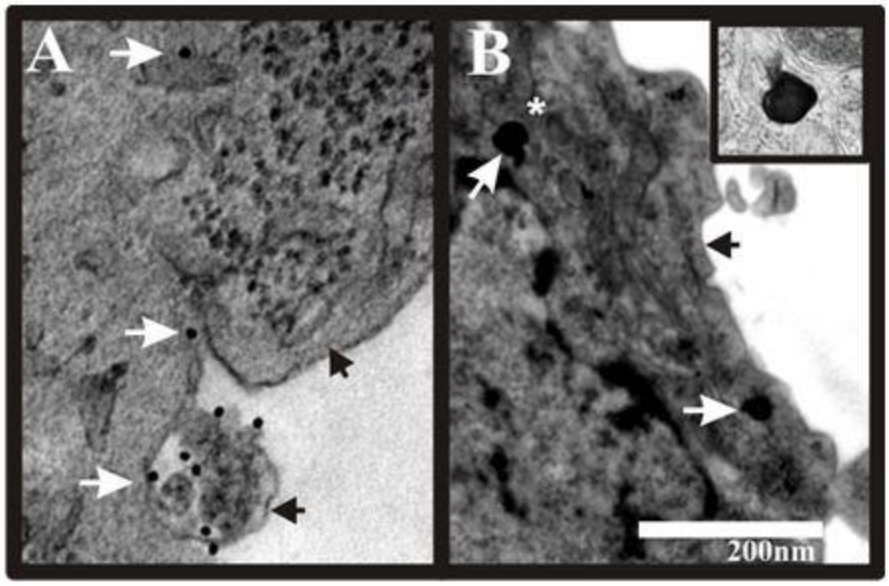

Figure 4.12. TEM images of PC12 cells incubated with spherical (A) and hollow (B) gold nanoparticles. Insert: an enlarged image of a hollow gold NP marked by the asterisk; White arrows: point out the gold nanoparticles, black arrows: show the membrane of the cell.

The NP size and surface chemistry determine the way NPs interact with the cellular membrane, hence the pathway involved in their uptake. The pathway and mechanism of NP entry could be by macropinocytosis, receptor mediated endocytosis (clathrin- or caveolae-mediated), clathrin- or caveolae-independent, as well as directly via passive diffusion. It has been suggested that the major mechanism of uptake involved is the receptor mediated endocytosis [8], though it has to be noted that this is highly dependent on the experimental conditions employed in a particular study, including the type of cells involved. The rate and extent of NP endocytosis depend on the size of the NP, as well as on the type of the cell.

As mentioned earlier, ICP-MS measurements of the amount of gold found within the neuron-like cells would enable us to draw solid conclusions by making quantitative comparisons between these two different gold NPs. In addition, critical evaluation of the information found can be done with the data currently found in literature by other research groups. For example, in [7] it was suggested that the free energy during NP endocytosis required for NP interaction with the membrane receptors, (and for the recruitment of these receptors on the site enclosing the NPs) was considered to be more in bigger NPs (74 nm) than smaller ones (14 nm and 50 nm). Also, in a different type of cell (human umbilical vein

endothelial cells) spherical gold NPs (15 nm) were found at higher concentrations within cells compared to hollow gold (100 nm) [10].

Furthermore, other cellular processes involved in NP endocytosis or even exocytosis, could not be specifically defined at this stage. Further investigations are needed in order to identify the exact cellular pathway involved, for example by assessing the NP uptake by blocking specific pathways. This information will enable us to construct a complete picture regarding the NP uptake and intracellular distribution of gold NPs within a neuron cell.

4.4 Cellular fate of Tet1-functionalised gold nanoparticles in PC12 cells

Another part of the investigation about gold NP-neuron interaction, involved the exposure of differentiated PC12 cells to NPs tagged with lysine terminated-Tet1 neuron specific targeting peptide. It was hypothesised that peptide-functionalised NPs would readily enter the cell; henceforth the fate of a large amount of NPs would be observed, however without triggering any signalling pathways [34, 48]. In an *in vitro* system there are time limitations for carrying out an experiment, hence peptide functionalised NPs were designed in an attempt to 'model' the exposure of cells to a large amount of NPs, as a consequence of a constant long term exposure to these NPs.

As mentioned previously, the surface chemistry of the NPs determines the way NPs interact with the membrane of the cell, thus the pathway involved in their uptake. In the case of the peptide-functionalised NPs, the Tet1 peptide has a high affinity and specifically binds to the Gtb1 (trisialoganglioside clostridial toxin) receptors, which are readily expressed on the membranes of these neuron-like cells [49]. An illustration of a lysine terminated Tet1-functionalised NP interacting with Gtb1 on the cell surface membrane is shown in the figure below. Hence, it is suggested that the majority of the Tet1 functionalised NPs would have entered the cell via the Gtb1 receptor-mediated pathway [49].

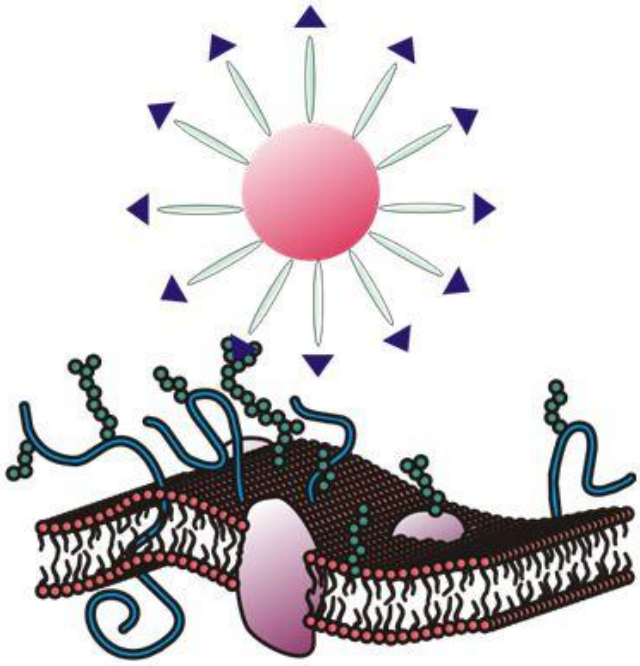

Figure 4.13. Interaction of Tet1 functionalised NP with the cell surface membrane.

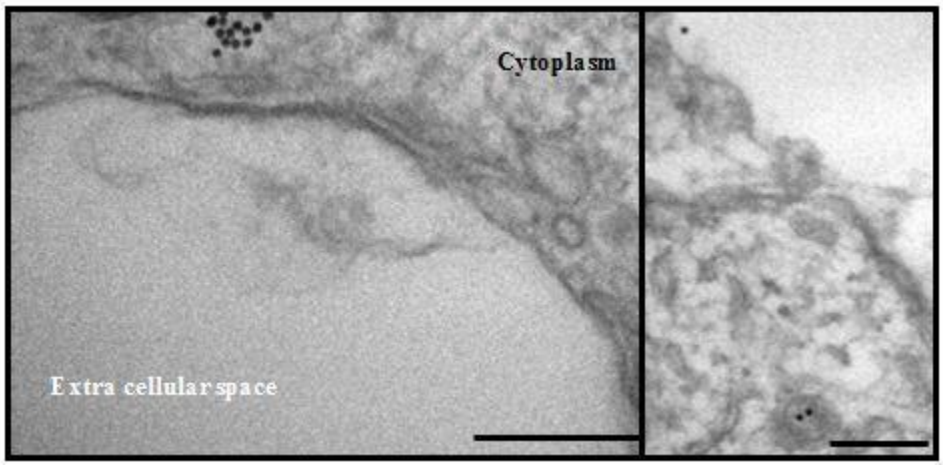

Figure 4.14. TEM images of PC12 neuron-like cells treated with OEG capped NPs. Scale bar = 200 nm

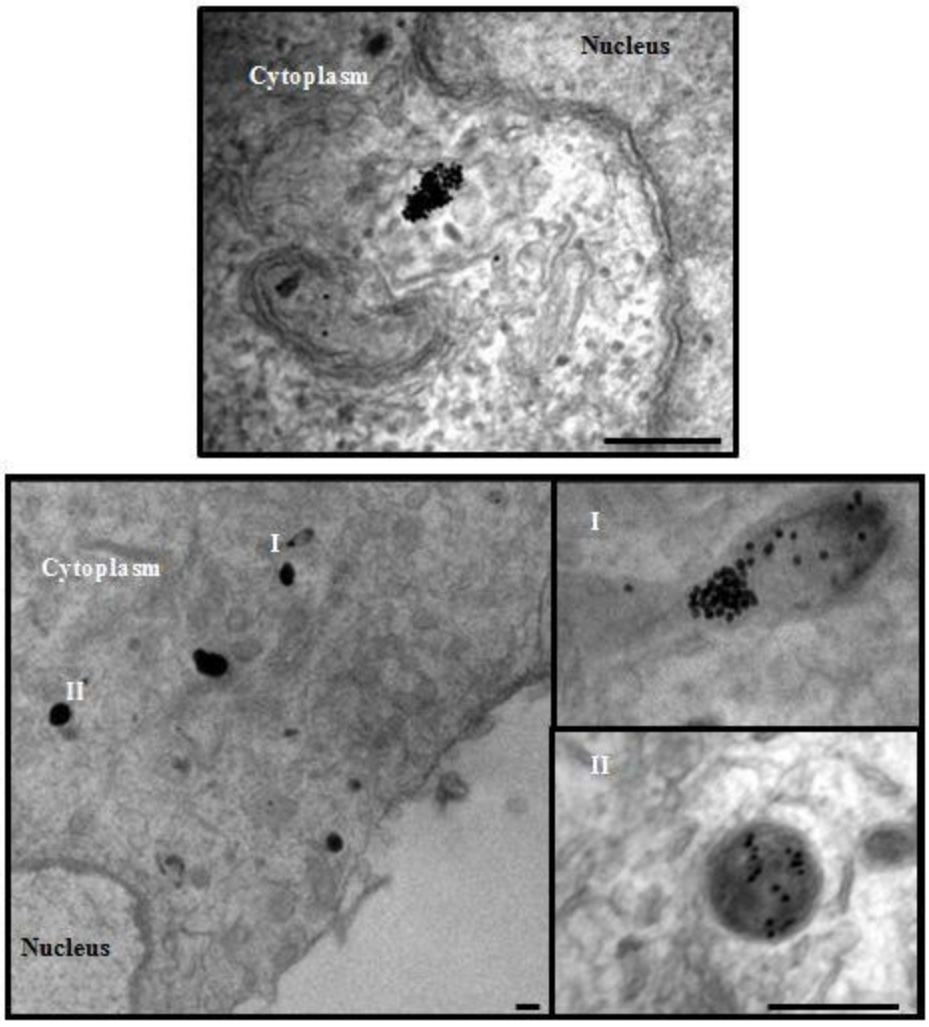

Figure 4.15. TEM images of PC12 neuron cell line that were treated with Tet1-functionalised NPs. Scale bars = 200 nm.

Differentiated PC12 neurons were incubated for one hour with spherical gold NPs. OEG-capped particles were taken up by the neuron-like cells non-specifically, and they were located in the cytoplasm of cells (see Section 4.3). On the other hand, Tet1-functionalised NPs seemed to be taken up more readily by cells. Nevertheless, ICP-MS measurements are required in order to validate and confirm these qualitative observations.

A close observation of the TEM images, in Figure 4.15, reveals something interesting, that the internalized Tet1-functionalized gold NPs seemed to be found in small groups trapped within sub-cellular organelles. It can be suggested that the cell actively collected these NPs into these organelles, after they have entered the cells.

Comparing the images of OEG-capped NPs and lysine terminatedTet1-functionalised NPs it can be inferred that these loaded vesicles were transported to the inner part of the cell around the cell soma particularly close to the perinuclear region (the area around the cell nucleus). In [50] a similar observation was noted, when vesicles containing peptide (Tat)-functionalised Quantum Dots (in HeLa cells) followed a similar path, from the periphery of the cell to its perinuclear region via an active transport cellular process. Furthermore, this observation was also consistent with previous studies with PC12 cells [35], as well as GI-1 glioma cells [51]. Nevertheless, further experiments have to be conducted to shed more light in the gold NP- neuron cell interaction (particularly about the events taking place within the cell following the NP uptake) in order to make solid and constructive comparisons with other studies like the ones mentioned above.

The diffusion of such large vesicles through the crowded and dense cytoplasm is minimal, therefore it is suggested that this limitation was overcomed by a retrograde transport system involving the hijacking of the cellular machinery (such the microtubule network, dynein motor protein, etc.) [34, 50]. As it was mentioned in Chapter 2, Tet1 peptide has similar binding characteristics to that of tetanus toxin. Tetanus toxin has the ability to bind to the neurons in the periphery and by retrograde transport is transported to the motor neurons [34]. Similarly, it was suggested that the Tet1 peptide enabled the peptide functionalised NPs to be actively transported to the perinuclear region of the cell.

Moreover, a close observation of the PC12 cells following exposure to the peptide-functionalised NPs under the light microscope (before they were processed for TEM), revealed that there was not any significant change in the phenotype of the cells. However, in order to study any changes in the functional processes of the cell as a consequence of the presence of NPs within the cell both in low (OEG-capped NPs) or high numbers (lysine terminated Tet1-functionalised NPs), further investigations are required involving detection of proteins that their expression is altered during a stress response by western-blot analysis.

4.5 Hyperspectral darkfield imaging of single hollow gold NPs for biomedical applications

Another study with neuron-like cells was carried out whereby individual hollow gold NPs were imaged within a biological sample, as a part of the investigation regarding the interaction of inorganic NPs with cells. The study involved differentiated SH-SY5Y cells that were exposed to hollow gold Tet1-functionalised NPs. The development of this technique by the Muskens group is very important, as hyperspectral darkfield imaging can be extended to live cell studies. For example, for studying NP cellular uptake and fate, in which currently phototoxicity is considered to be a limiting factor. Such studies will provide us with new insight information regarding the uptake and handling of NPs by the cell, as well as employing single NPs as spectral sensors of a particular sub-cellular activity.

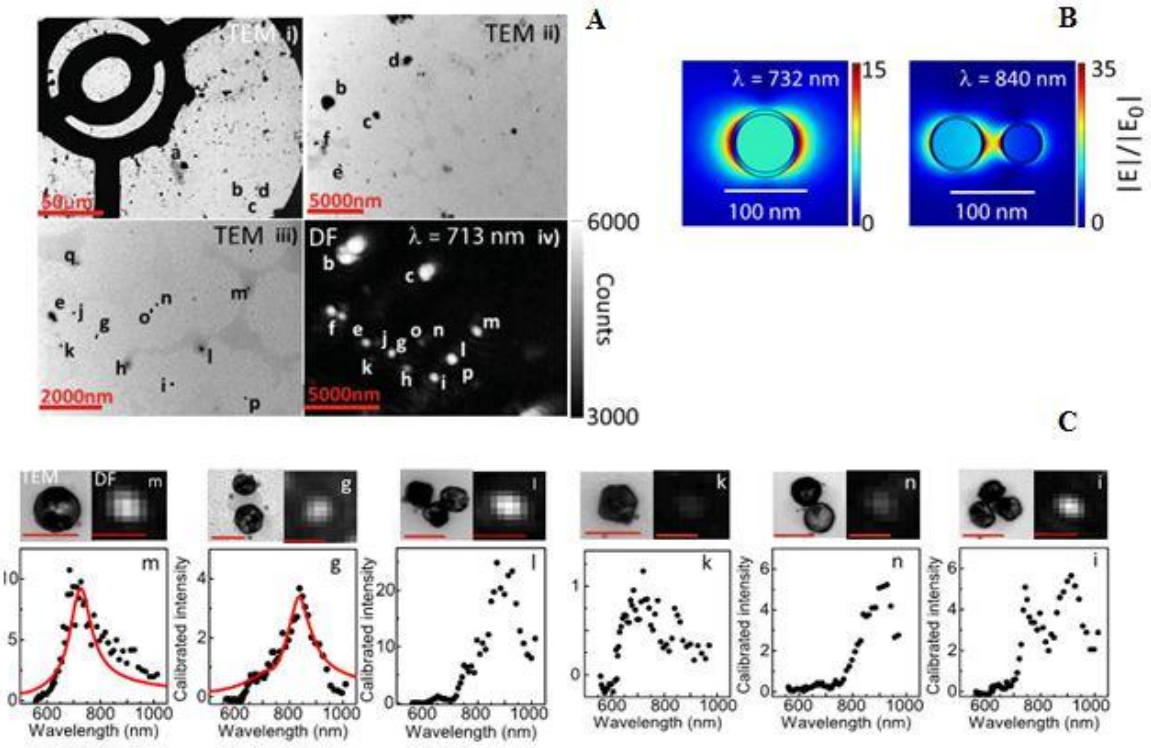

Figure 4.16. Hyperspectral measurements of hollow gold nanoparticles. Image taken from [41]

The TEM images of OEG-capped hollow gold NPs (on marked TEM grids), such as in Figure 4.16 A i-iii, were correlated with the images taken with the hyperspectral darkfield setup with incident light wavelength of 713 nm (Figure 4.16iv) in order to detect individual

NPs. Looking at the images in Figure 4.16, it can be observed that there are individual NPs (*m*, *k*), dimmers (*g*, *n*), trimmers (*l*, *i*) and the rest NPs on the grid are in clusters. The details of the setup parameters can be found in [41].

The resonance of *m*, single hollow gold NP, at 685 nm ±10 nm is in agreement with that of hollow gold [52] in other imaging studies with single NPs. The spectral response (red line) was qualitatively reproduced, using a numerical model for a single hollow gold NP. The TEM image was used to calculate the NP diameter, and the shell thickness was optimized to achieve agreement with the spectral resonance position. This is because the shell thickness varied amongst the NPs. Furthermore, the morphology of most NPs deviates from that of a perfect sphere, which makes the quantitative analysis of the spectral response even more complicated.

In Figure 4.16 C, the mode profile which corresponds to the spectral resonance peak of NP *m* is presented. The resonance could be due to the NPs dipolar mode, with a local field enhancement of one order of magnitude. On the other hand, NP *k* response was not as strong as NP *m*. This discrepancy arises from the difference in the NPs sizes. The scattering cross-section scales with the square of the particle volume in small NPs, hence even a slight size difference could have as a consequence a large difference in the intensity detected. The setup by Muskens group is sensitive enough to detect individual NPs smaller than 50 nm, with quite short integration time and good signal/noise ratio.

In comparison to the individual NPs, when the NPs are in groups of two or three (such as in *n*, *i* and *l* clusters), a red shift in the spectral response was observed, as expected for strongly interacting nanoshells [53]. In particular, the NP cluster *i* showed a complex spectral response with multiple resonances, which could be attributed to the discrepancy in the NP size. The theoretical spectrum (in Figure 4.16 B) for the NP cluster *g* resulted from modelling the two NPs.

4.5.1 Hyperspectral darkfield measurements of hollow gold nanoparticles interacting with SH-SY5Y cells

In the previous sections of Chapter 4, an investigation using transmission electron microscopy for studying NP-cell interaction was presented, however this technique is

considered costly and time consuming compared to other imaging techniques, such as hyperspectral darkfield microscopy. Furthermore, the optical properties of gold NPs enable the study of single NPs when using the latter technique.

The hyperspectral darkfield microscope designed by Ms Tasha Fairbairn was used to study the interaction of single hollow gold NPs with SH-SY5Y cells. SH-SY5Y cells were exposed, for one hour, to hollow gold NPs functionalised with lysine terminated-Tet1 peptide. The images of cells obtained using brightfield, DAPI fluorescence and hyperspectral darkfield scattering (at 713 nm) microscopy, were overlayed. This was done in an attempt to study how the NPs interacted with the cells (see Figure 4.15). In the spatial map, there is a clear contribution of darkfield intensity, which is associated with the position of the cell. Looking at Figure 4.16 it can be observed that four single bright spot areas were chosen for more extensive spectroscopic analysis (spectra *i* – *iv*). Interestingly, the spectra of *i*, *iii*, and *iv* showed a peak around 700 nm, consistent with the approximate spectral resonance and intensity of single hollow gold NPs as determined from the correlative transmission electron microscopy study. Furthermore, the spectrum obtained for the bright spot area *ii* had a complex red-shifted response –compared to the individual NPs- as expected for a typical response for a group of two or more NPs.

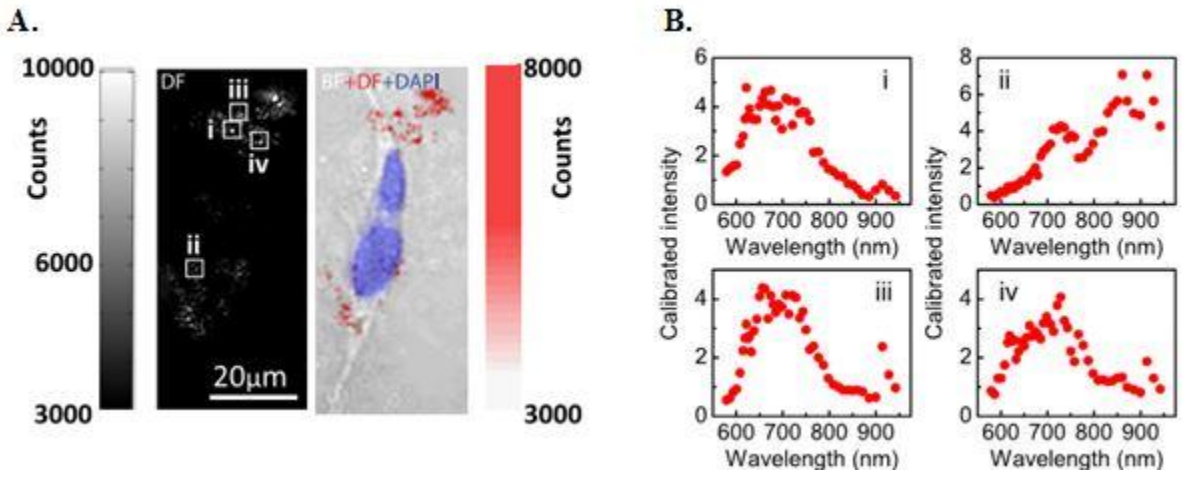

Figure 4.17. A. Darkfield image at 713 nm, and B. a combined false colour image showing darkfield, DAPI fluorescence and brightfield images of a SH-SY5Y cell that has been incubated with hollow gold nanoparticles for 1 h are shown along with spectra (i)–(iv), taken from different bright spots indicated on the darkfield image. Integration time: 0.1 s per image. Images taken from [41].

The interaction of NPs and their uptake by the cell-as mention in previous chapters- depends on the capping and functionalization of their surface area. For example, NPs that are OEG-capped when exposed to cells are taken up by cells non-specifically. On the other hand, NPs that are functionalised with a cell specific binding peptide, such as the Tet1, possibly a receptor-mediated endocytosis is promoted.

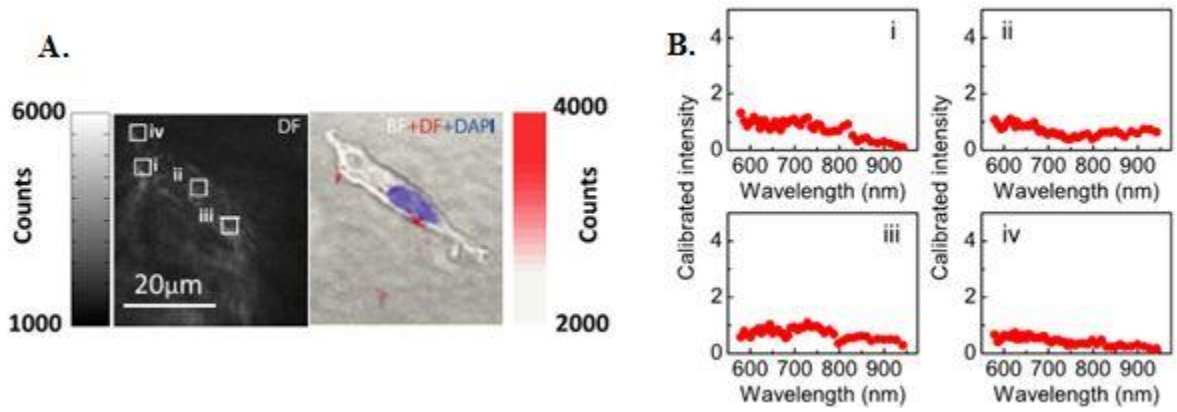

Figure 4.18. A. Darkfield image at 713 nm, and B. a combined false colour image showing darkfield, DAPI fluorescence and brightfield images of a control SH-SY5Y cell that was not been incubated with hollow gold nanoparticles are shown along with spectra (i)–(iv), taken from different bright spots indicated on the darkfield image. Integration time: 0.1 s per image. Images taken from **[41]**.

In Figure 4.18, looking at the image of the cell which was not incubated with hollow gold NPs (control sample), there was some intensity when the sample was viewed in darkfield. However, the intensity was lower and smooth over the control sample, without any sharp features present. This light intensity could be attributed to the light intensity scattered from the cell itself. The spectra *i-iv* shown in Figure 4.18, do not have the characteristic peaks of NP resonances and are about five times lower than the signals obtained from single NPs. Therefore, this light intensity can be clearly differentiated from the NP signals.

The results obtained from this study suggest that the peptide-functionalised NPs seemed to interact with the cells after a short time of incubation, compared to the control sample. However, at this point no conclusion can be drawn where exactly the NPs are found relative to the cell, henceforth, more experiments are required, whereby the cytoskeleton of the cell together with a few subcellular organelles could be fluorescently labelled.

Furthermore, the illumination intensity used was considered to be low (<0:5 W/cm^2) and safe to be used for future studies with living cells and metallic NPs [10]. In addition, a different investigation could be conducted using single hollow gold NPs as spectral sensors of a particular activity within the cell, for example for studying a specific cell signalling pathway [54].

Chapter 5. Conclusions

In the last few decades, advances in nanoscience have resulted in the production and use of inorganic NPs. These NPs have been used commercially for a range of applications, particularly in the biomedical field, based on their exceptional chemical and physical properties, which are very different to that in the larger scale (see Chapter 2).

Nevertheless, in order to encourage the use of inorganic NPs in our everyday life, and more specifically in the clinical setting, our understanding regarding the NP interaction with the cells following NP exposure, it is very important [9]. This was the motivation for the work carried out in this thesis, as described in Chapter 1.

Firstly, this investigation involved the synthesis of spherical and hollow gold NPs (see Sections 2.4 and 3.1) which were then capped with water soluble organic ligands, such as OEG. The resulting OEG-capped NPs were then functionalised by attaching a specific targeting peptide, lysine terminated-Tet1, on their organic corona (see Sections 2.5 and 3.2). The surface modification of the NPs by the aforementioned ligands, was carried out so that the NPs could be employed in the biological investigations carried out in this work.

Two types of neuron-like cell lines were employed, PC12 and SH-SY5Y cells, which are considered to be good models for neurobiological investigations and share many characteristics with primary neurons. These neuron-like cells were exposed to the synthesised gold NPs, and the fate of these NPs within the cells was studied by using imaging techniques, such as transmission electron (see Sections 4.3 and 4.4) and hyperspectral darkfield microscopy (see Section 4.5).

In Section 4.3 it was shown from the TEM images that spheres and hollow gold NPs were found within the PC12 cells, indicating that they were able to traverse through the cell membrane. Nevertheless, the pathway and cellular processes involved could not be specifically defined at this stage of the investigation. Further and extensive studies will enable us to create a complete profile regarding the cellular pathways involved in cellular uptake, distribution, as well as, exocytosis of NPs.

Furthermore, the investigation about the interaction of PC12 cells with peptide functionalised spherical gold NPs was presented in Section 4.4. The peptide functionalised NPs were used to target the GTb1 receptors that are expressed readily on the neuron-cell lines employed in this project. The uptake and distribution of the lysine terminated Tet1-

functionalised NPs and OEG-capped NPs were different. Lysine terminated Tet1-functionalised NPs uptake seemed to be greater compared to OEG-capped NPs, and they were transported to the inner part of the cell around its perinuclear region. A study using images obtained from TEM, can give solid evidence on the location of the NPs relative to the cell (as the cell with its sub-cellular structures can be clearly distinguished). On the other hand, a TEM study with various factors under investigation would be time consuming, and within the time frame of this thesis it was not possible. Therefore, future experiments involving fluorescently tagged NPs would give us an inside on the cellular events that take place following NP exposure, over time. In addition, imaging techniques of non-fluorescent metallic NPs could be employed, such as the hyperspectral darkfield microscopy shown earlier in Section 4.5. Furthermore, western blot analysis of proteins involved in a cell stress response could be conducted in future experiments. Such an investigation would show us whether the cell is under a stress when it is exposed to gold NPs, and how the cell deals with such an 'insult' overtime.

The application of the hyperspectral darkfield microscope designed by the Muskens group for imaging of single hollow gold NPs on a TEM grid and in a biological sample with fixed SH-SY5Y cells, was also presented in this Thesis. The illumination intensity used was <0:5 W/cm^2, which is considered to be a very positive parameter for future studies with living cells and metallic NPs [10]. In addition, more and different investigations could be conducted with single hollow gold NPs that could serve as spectral sensors of a particular activity within the cell, in order to shed some light in the events taking place during, for example a cell signalling pathway [54].

References

[1] K. S. Henthorn, M. S. Roux, C. Herrera, and L. S. Goldstein, "A role for kinesin heavy chain in controlling vesicle transport into dendrites in Drosophila," *Mol Biol Cell.*, vol. 22, no. 21, pp. 4038-4046, 2011.

[2] S. Jain, D. G. Hirst, and J. M. O'Sullivan, "Gold nanoparticles as novel agents for cancer therapy," *Br J Radiol*, vol. 85, no. 1010, pp. 101-113, 2012.

[3] A. D. Maynard, "NANOTECHNOLOGY: A Research Strategy for Addressing Risk," *Project on Emerging Nanotechnologies-Review*, 2006.

[4] F. R. Cassee, E. C. van Balen, C. Singh, D. Green, H. Muijser, J. Weinstein, and K. Dreher, "Exposure, health and ecological effects review of engineered nanoscale cerium and cerium oxide associated with its use as a fuel additive," *Crit Rev Toxicol*, vol. 41, no. 3, pp. 213-229, 2011.

[5] J. S. Tsuji, A. D. Maynard, P. C. Howard, J. T. James, C. W. Lam, D. B. Warheit, A. B. Santamaria, "Research strategies for safety evaluation of nanomaterials, part IV: risk assessment of nanoparticles," *Toxicol Sci*, vol. 89, no. 1, pp. 42-50, 2006.

[6] M. E. Davis, J. E. Zuckerman, C. H. J. Choi, D. Seligson, A. Tolcher, C. A. Alabi, Y. Yen, J. D. Heidel, and A. Ribas, "Evidence of RNAi in humans from systemically administered siRNA via targeted nanoparticles," *Nature*, vol. 464, no. 7291, pp. 1067-1070, 2010.

[7] B. D. Chithrani, and W. C. Chan, "Elucidating the Mechanism of Cellular Uptake and Removal of Protein-Coated Gold Nanoparticles of Different Sizes and Shapes," *Nanoletters*, vol. 7, no. 6, pp. 1542-1550, 2007.

[8] L. Y. Chou, K. Ming, and W. C. Chan, "Strategies for the intracellular delivery of nanoparticles," *Chem Soc Rev,* vol. 40, no. 1, pp. 233-245, 2011.

[9] E. C. Dreaden, A. M. Alkilany, X. Huang, C. J. Murphy, and M. A. El-Sayed, "The golden age: gold nanoparticles for biomedicine," *Chem. Soc. Rev.,* vol. 41, p. 2740–2779, 2012.

[10] D. Bartczak, O. L. Muskens, S. Nitti, T. Sanchez-Elsner, T. M. Millar, A. G. Kanaras, "Interactions of Human Endothelial Cells with Gold Nanoparticles of Different Morphologies," *Small,* vol. 8, no. 1, pp. 122-130, 2012.

[11] E. Hutter, S. Boridy, S. Labrecque, M. Lalancette-Hébert, J. Kriz, F. M. Winnik, and D. Maysinger, "Microglial Response to Gold Nanoparticles," *ACS Nano,* vol. 4, no. 5, pp. 2595-2606, 2010.

[12] Arnida, A. Malugin, and H. Ghandehari, "Cellular uptake and toxicity of gold nanoparticles in prostate cancer cells: a comparative study of rods and spheres," *J Appl Toxicol,* vol. 30, no. 3, pp. 212-217, 2010.

[13] S. K. Libutti, G. F. Paciotti, A. A. Byrnes, H. R. Jr Alexander, W. E. Gannon, M. Walker, G. D. Seidel, N. Yuldasheva, and L. Tamarkin, "Phase I and pharmacokinetic studies of CYT-6091, a novel PEGylated colloidal gold-rhTNF nanomedicine," *Clin Cancer Res,* vol. 16, no. 24, pp. 6139-6149, 2010.

[14] J. Chen, J. Zhu, H.-H. Chob, K. Cuia, F. Lia, X. Zhoua, J. T. Rogersb, S. T.C. Wonga, and X. Huanga, "Differential cytotoxicity of metal oxide nanoparticles," *Journal of Experimental Nanoscience,* vol. 3, no. 4, pp. 321-328, 2008.

[15] S. M. Hussain, A. K. Javorina, A. M. Schrand, H. M. Duhart, S. F. Ali, and J. J. Schlager, "The interaction of manganese nanoparticles with PC-12 cells induces dopamine depletion," *Toxicol Sci,* vol. 92, no. 2, pp. 456-463, 2006.

[16] T. R. Pisanic, J. D. Blackwell, V. I. Shubayev, R. R. Fiñones, and S. Jin, "Nanotoxicity of iron oxide nanoparticle internalization in growing neurons," *Biomaterials,* vol. 28, no. 16, pp. 2572-2581, 2007.

[17] A. V. Kuznetsov, "Modelling transport of layered double hydroxide nanoparticles in axons and dendrites of cortical neurons," *Comput Methods Biomech Biomed Engin,* vol. 38, no. 5, 2011.

[18] L. M. Mendonça, G. C. Dos Santos, G. A. Antonucci, A. C. Dos Santos, L. Bianchi Mde, L. M. Antunes, "Evaluation of the cytotoxicity and genotoxicity of curcumin in PC12 cells," *Mutat Res,* vol. 675, no. 1-2, pp. 29-34, 2009.

[19] L. A. Greene, and A. S. Tischler, "Establishment of a noradrenergic clonal line of rat adrenal pheochromocytoma cells which respond to nerve growth factor," *Proc. Natl. Acad. Sci,* vol. 73, no. 7, pp. 2424-2428, 1976.

[20] Y.-S. Hsiao, C.-C. Lin, H.-J. Hsieh, S.-M. Tsai, C.-W. Kuo, C.-W. Chu, and P. Chen , "Manipulating location, polarity, and outgrowth length of neuron-like pheochromocytoma (PC-12) cells on patterned organic electrode arrays," *Lab Chip,* vol. 11, no. 21, pp. 3674-3680, 2011.

[21] M. Encinas, M. Iglesias, Y. Liu, H. Wang, A. Muhaisen, V. Ceña, C. Gallego, and J. X. Comella , "Sequential Treatment of SH-SY5Y Cells with Retinoic Acid and Brain-Derived Neurotrophic Factor Gives Rise to Fully Differentiated, Neurotrophic Factor-Dependent Human Neuron-Like Cells," *Journal of Neurochemistry,* vol. 75, no. 3, pp. 991-1003, 2000.

[22] A. Jämsä, K. Hasslund, R. F. Cowburn, A. Bäckström, and M. Vasänge, "The retinoic acid and brain-derived neurotrophic factor differentiated SH-SY5Y cell line as a model for Alzheimer's disease-like tau phosphorylation," *Biochem Biophys Res Commun,* vol. 319, no. 3, pp. 993-1000, 2004.

[23] K. L. Kelly, E. Coronado, L. L. Zhao, and G. C. Schatz, "The Optical Properties of Metal Nanoparticles: The Influence of Size, Shape, and Dielectric," *J. Phys. Chem. B,* vol. 107, no. 3, pp. 668-677, 2003.

[24] P. K. Jain, I. H. El-Sayed, and M. A. El-Sayed, "Au nanoparticles target cancer," *Nano Today,* vol. 2, pp. 18-29, 2007.

[25] M. A. Yurkin, and A. G. Hoekstra, "The discrete dipole approximation: an overview and recent developments," *Quant Spectrosc Radiat Transf,* vol. 106, pp. 558-589, 2007.

[26] M. Hu, J. Chen, Z. Y. Li, L. Au, G. V. Hartland, X. Li, M. Marqueze, and Y. Xia, "Gold nanostructures: engineering their plasmonic properties for biomedical applications," *Chem. Soc. Rev.,* vol. 35, p. 1084–1094, 2006.

[27] Y. Sun, and Y. Xia , "Mechanistic Study on the Replacement Reaction between Silver Nanostructures and Chloroauric Acid in Aqueous Medium," *Journal of the Americal Chemical Society,* vol. 126, no. 12, pp. 3892-3901, 2004.

[28] S. Kumar, K. S. Gandhi, and R. Kumar, "Modeling of Formation of Gold Nanoparticles by Citrate Method," *Ind. Eng. Chem. Res.,* vol. 46, pp. 3128-3136, 2007.

[29] A. G. Kanaras, F. S. Kamounah, K. Schaumburg, C. J. Kiely, and M. Brust, "Thioalkylated tetraethylene glycol: a new ligand for water soluble," *Chemical Communications,* no. 20, pp. 2294-2295, 2002.

[30] G. T. Hermanson,, Bioconjugate Techniques, 2nd ed., Elsevier Inc., 2008.

[31] Zhang, "Potential Use of Polymersomes and Lipid Nanocapsules as Therapeutic Carriers in the Rat Inner Ear," *PhD Thesis,* 2011.

[32] J. L. Liu, Q. Teng, M. Garrity-Moses, T. Federici, D. Tanase, M. J. Imperiale, and N. M. Boulis, "A novel peptide defined through phage display for therapeutic protein and vector neuronal targeting," *Neurobiol Dis,* vol. 19, no. 3, pp. 407-418, 2005.

[33] T. Federici, J. K. Liu, Q. Teng, M. Garrity-Moses, J. Yang, and N. M. Boulis, "Neuronal affinity of a C7C loop peptide identified through phage display," *J Drug Target,* vol. 14, no. 5, pp. 263-271, 2006.

[34] E. J. Kwon, J. M. Bergen, I. K. Park, and S. H. Pun, "Peptide-modified vectors for nucleic acid delivery to neurons," *Journal of Controlled Release,* vol. 132, p. 230–235, 2008.

[35] I.-K. Park, J. Lasiene, S.-H. Chou, P. J. Horner, and S. H. Pun, "Neuron-specific delivery of nucleic acids mediated by Tet1-modified poly(ethylenimine)," *J Gene Med,* vol. 9, no. 8, pp. 691-702, 2007.

[36] M. A. Van Dijk, A. L. Tchebotareva, M. Orrit, M. Lippitz, S. Berciaud, D. Lasne, L. Cognet, and B. Lounis, "Absorption and scattering microscopy of single metal nanoparticles," *Phys. Chem. Chem. Phys.,* vol. 8, p. 3486–3495, 2006.

[37] J. Mock, M. Barbic, D. R. Smith, D. A. Schultz, and S. Schultz, "Shape effects in plasmon resonance of individual colloidal silver nanoparticles," *J. Chem. Phys.,* vol. 116, p. 6756–6759, 2002.

[38] C. Sonnichsen, B. M. Reinhard, J. Liphardt, and A. P. Alivisatos, "A molecular ruler based on plasmon coupling of single gold and silver nanoparticles," *Nat.Biotechnol.,* vol. 23, p. 741–745, 2005.

[39] J. N. Anker, W. P. Hall, O. Lyandres, N. C. Shah, J. Zhao, and R. P. Van Duyne, "Biosensing with plasmonic nanosensors," *Nat. Mater.,* vol. 7, p. 442–453, 2008.

[40] Z. Krpetic, P. Nativo, V. See, I. A. Prior, M. Brust, and M. Volk, "Inflicting Controlled Nonthermal Damage to Subcellular Structures by Laser-Activated Gold Nanoparticles," *Nano Lett.,* vol. 10, p. 4549–4554, 2010.

[41] N. Fairbairn, A. Christofidou, A. G. Kanaras, T. A. Newman, and O. L. Muskens, "Hyperspectral darkfield microscopy of single hollow gold nanoparticles for biomedical

applications," *Phys. Chem. Chem. Phys.,* 2013.

[42] G. K. Mc Evoy, "Drug Information The American Hospital Formulary Service," *IPCS INCHEM, American Society of Health-System Pharmacists, Inc., MD.,* 1993.

[43] M. S. Ming-Li, Towards the electrical stimulation of PC12 cells, Saskatoon, Canada: University of Saskatchewan, 2012.

[44] I. O. Sosa, C. Noguez, and R. G. Barrera, "Optical Properties of Metal Nanoparticles with Arbitrary Shapes," *J. Phys. Chem. B* , vol. 107, pp. 6269-6275, 2003.

[45] P. K. Jain, K. S. Lee, I. H. El-Sayed, and M. A. El-Sayed, "Calculated Absorption and Scattering Properties of Gold Nanoparticles of Different Size,Shape, and Composition: Applications in Biological Imaging and Biomedicine," *J. Phys. Chem. B* , vol. 110, pp. 7238-7248, 2006.

[46] V. Sanz, J. Conde, Y. Hernandez, P. V. Baptista, M. R. Ibarra, and J. M. de la Fuente, "Effect of PEG biofunctional spacers and TAT peptide on dsRNA loading on gold nanoparticles," *J Nanopart Res,* vol. 14, no. 917, pp. 1-9, 2012.

[47] D. Bartczak, T. Sanchez-Elsner, F. Louafi, T. M. Millar, A. G. Kanaras, "Receptor-Mediated Interactions between Colloidal Gold Nanoparticles and Human Umbilical Vein Endothelial Cells," *Small,* vol. 7, no. 3, pp. 388-394, 2011.

[48] P. S. Fishman, and D. R. Carrigan, "Retrograde transneuronal transfer of the C-fragment of tetanus toxin," *Brain Research,* vol. 406, no. 1-2, p. 275–279, 1987.

[49] Y. Zhang, W. Zhang, A. H. Johnston, T. A. Newman, I. Pyykkö, and J. Zou, "Targeted delivery of Tet1 peptide functionalized polymersomes to the rat cochlear nerve," *International Journal of Nanomedicine,* vol. 7, p. 1015–1022, 2012.

[50] G. Ruan, A. Agrawal, A. I. Marcus, and S. Nie, "Imaging and Tracking of Tat Peptide-Conjugated Quantum Dots in Living Cells: New Insights into Nanoparticle Uptake

Intracellular Transport, and Vesicle Shedding," *J. AM. CHEM. SOC.,* vol. 129, pp. 14759-14766, 2007.

[51] A. Mathew, T. Fukuda, Y. Nagaoka, T. Hasumura, H. Morimoto, Y. Yoshida, T. Maekawa, K. Venugopal, and D. S. Kumar, "Amyloid-binding aptamer conjugated curcumin-PLGA nanoparticle for potential use in Alzheimer's disease.," *BioNano Science,* vol. 2, no. 2, pp. 83-93, 2012.

[52] A. M. Schwartzberg, T. Y. Olson, C. E. Talley, and J. Z. Zhang, "Synthesis, Characterization, and Tunable Optical Properties of Hollow Gold Nanospheres," *J. Phys. Chem. B,* vol. 110, p. 19935–19944, 2006.

[53] L. V. Brown, H. Sobhani, J. B. Lassiter, P. Nordlander, and N. J. Halas, "Heterodimers: Plasmonic Properties of Mismatched Nanoparticle Pairs," *ACS Nano,* vol. 4, p. 819–832, 2010.

[54] Y. Jun, S. Sheikholeslamia, D. R. Hostetter, C. Tajon, C. S. Craik, and A. P. Alivisatos, "Continuous imaging of plasmon rulers in live cells reveals early-stage caspase-3 activation at the single-molecule level," *Proc. Natl. Acad. Sci,* vol. 106, p. 17735–17740, 2009.

[55] S. Sun, H. Zeng, D. B. Robinson, S. Raoux, P. M. Rice, S. X. Wang, and G. Li, "Monodisperse MFe2O4 (M) Fe, Co, Mn) Nanoparticles," *JACS Communications,* vol. 126, pp. 3892-3901, 2004.

Appendix

A1. Spherical manganese ferrite nanoparticles

Manganese ferrite NPs were prepared by a modified method developed by Sun [55]. Iron (III) acetyl acetoate (0.70 g), manganese (II) acetyl acetoate (0.30 g), 1, 2 hexadecanediol (2.50 g), dodecylamine (1.27 g), lauric acid (1.10 g) and benzyl ether (20 ml) were mixed at 140 ^{o}C and under nitrogen, until they were completely dissolved. The reaction mixture was vigorously mixed at 140 ^{o}C for one hour (step one), then at 210 ^{o}C for two hours (step two; nucleation step) and finally at 300 ^{o}C for one hour (step three). The colour of the reaction mixture changed from bright red to dark brown. Once the reaction was completed the solution was poured into ice-cold glass vials filled with ethanol, isopropanol and acetone, and was centrifuged for 20 minutes (1000 rcf). The ethanol and isopropanol were used to dissolve the surfactant and the acetone to precipitate the NPs. The sample was purified by three further centrifugation/decantation steps. Acetone, isopropanol and ethanol were used to redisperse the pellet, except in the final purification step where toluene, was added. ICP-MS was used to quantify the concentration of the NPs.

The manganese ferrite NPs were transferred to water by coating their outer surface with poly(maleic anhydride-alt-1-octadecene) (the polymer). The NP: polymer ratio was 1:10. The NPs were precipitated using acetone. Then chloroform was added to dissolve the NPs and was evaporated under vacuum. Chloroform was added again in order to dissolve the NPs and the solution was sonicated at room temperature, for twenty minutes. The polymer solution (134 mM) was then added to the NPs. Another evaporation/dissolution step was carried out. The NPs were dissolved in borate buffer (pH 9) and the solution was sonicated at room temperature, for three hours. Once fully dissolved, the NP solution was precipitated by centrifugation (1500 rcf, 30 minutes) using 100 kDa molecular weight cut-off ultracentrifugation filtration membranes.

After the polymer coating, 0.5 mL of NPs solution was added to an ultracentrifuge tube with a sucrose gradient of 10 % to 60 %. The NP solution was separated from the free excess polymer into different bands by ultracentrifugation (25 000 rcf; 3 ½ h; 4 ^{o}C). The purified NP

solution band was extracted using a syringe and was further purified from sucrose by four purification steps (2 100 rcf; 12 minutes per step) using 100 kDa molecular weight cut-off ultracentrifugation filtration membranes. Borate buffer, pH 9, was added in each step.

In order to identify any free polymer present in the NP solution, gel electrophoresis was performed (60min; 100 mV; 1% agarose gel; 0.5x TBE buffer, pH 8).

A1.2. Manganese ferrite nanoparticles: Characterisation

The iron manganese oxide NPs were spherical (Figure A1.1) with an average size of 8 nm. Their size was altered by changing the time point and temperature of the nucleation step (second step) during the chemical synthesis. A delayed nucleation step or higher temperature (>210 ^{o}C) resulted in the formation of smaller NPs. The molar concentration of each element present in iron manganese oxide NPs, was determined by ICP-MS (before and after polymer coating). Furthermore, the purity of a polymer coated NP sample was qualitatively examined using electrophoretic analysis.

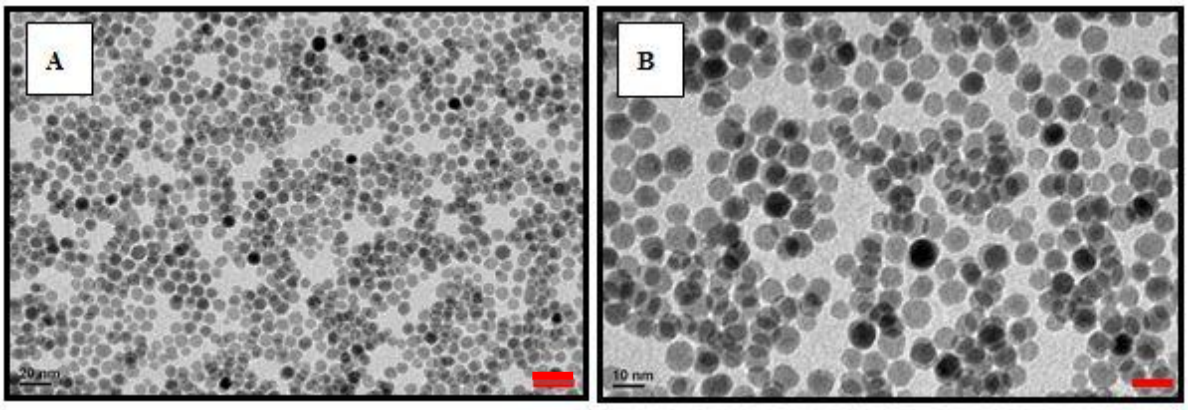

Figure A.1.1 A TEM image of FeMnO nanoparticle solution in toluene; scale bar = A: 20 nm and B: 10 nm.

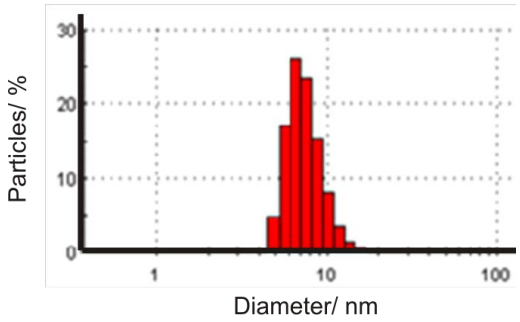

Figure A.1.2. Size distribution of the manganese ferrite NPs.

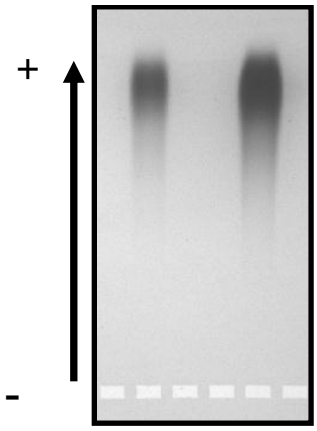

Figure A.1.3. Electrophoretic analysis of polymer coated, ultrapurified iron manganese oxide nanoparticles.

A2. Immunohistochemistry of beta-tubulin

The beta-tubulin in the cell cytoskeleton was fluorescently labelled with immunohistochemical techniques. The cells were washed twice with pre-warmed PBS and then fixed with 4 % PFA in PBS for 15 minutes (at room temperature). These were then washed three times with PBS-Tween (0.001 %), and blocked with 5 % normal goat serum for 30 minutes (at room temperature). The blocking solution was aspirated and the goat mouse beta tubullin primary antibody (prepared in 0.25 % normal goat serum, PBS-Tween, 1: 200) was added to the samples and left overnight (at 4 ^{o}C). The next day, the samples were washed three times with PBS-Tween (five minutes per wash). The secondary antibody, goat anti-mouse 488 nm (prepared in 0.25 % NGS, PBS-Tween) was added (in 1: 200) to the samples. Then the samples were washed and then mounted with DAPI and left to dry for approximately 24 hours (at room temperature in the dark).